

## Artificial intelligence forecasting models of uniaxial compressive strength



Arsalan Mahmoodzadeh<sup>a,\*</sup>, Mokhtar Mohammadi<sup>b</sup>, Hawkar Hashim Ibrahim<sup>c</sup>, Sazan Nariman Abdulhamid<sup>c</sup>, Sirwan Ghafoor Salim<sup>d</sup>, Hunar Farid Hama Ali<sup>a</sup>, Mohammed Kamal Majeed<sup>e</sup>

<sup>a</sup> Department of Civil Engineering, University of Halabja, Halabja, Kurdistan Region, Iraq

<sup>b</sup> Department of Information Technology, Lebanese French University, Erbil, Kurdistan Region, Iraq

<sup>c</sup> Civil Engineering Department, College of Engineering, Salahaddin University-Erbil, 44002 Erbil, Kurdistan Region, Iraq

<sup>d</sup> Sulaimani Polytechnic University, Technical College of Engineering, City Planning Department, Kurdistan Region, Iraq

<sup>e</sup> Faculty of Science, Department of Information Technology, Tishk International University, Kurdistan Region, Iraq

### ARTICLE INFO

#### Keywords:

Uniaxial compressive strength  
Artificial intelligence  
Geomechanical parameters  
Forecasting model

### ABSTRACT

The uniaxial compressive strength (UCS) is a vital rock geomechanical parameter widely used in rock engineering projects such as tunnels, dams, and rock slope stability. Since the acquisition of high-quality core samples is not always possible, researchers often indirectly estimate these parameters. The main objective of the present study is to evaluate the performance of the long short term memory (LSTM), deep neural networks (DNN), K-nearest neighbor (KNN), Gaussian process regression (GPR), support vector regression (SVR), and decision tree (DT) to predict the UCS of different rock types of Claystone, Granite, Schist and Sandstone, Travertine, Limestone, Slate, Dolomite and Marl acquired from almost all quarry locations of Iran. 170 data sets, including porosity (n), Schmidt hammer (SH), P-wave velocity ( $V_p$ ), and point load index ( $Is_{(50)}$ ) were applied in the methods. Finally, a comparison was made between the results made by the prediction methods. To assess the performance ability of the applied methods, the 5-fold cross-validation (CV) was considered. The results proved that computational intelligence approaches are capable of predicting UCS. On the whole, the GPR with a correlation coefficient ( $R^2$ ) of 0.9955 and a route mean square error (RMSE) of 0.52169, performs best. Lastly, the UCS prediction intelligence methods were ordered as GPR, DT, SVR, LSTM, DNN and KNN, respectively.

### Introduction

Intact rock behavior is profoundly and greatly determined by the Uniaxial Compressive Strength (UCS), both in the preliminary and the final design phases of rock and geotechnical engineering, in the projects such as tunneling, rock mass excavation, dam construction, slope stability and even creating infrastructure foundations [39,16,7,18,19,47]. The main approach for evaluating UCS and E is to check the specimens in the laboratory according to procedures proposed by the American Society for Testing Materials (ASTM) and the International Society for Rock Mechanics (ISRM) [78]. Nonetheless, laboratory experiments as direct approaches for estimating tensile strength are not known to be time-and cost-effective [41]. In addition, exposure to an adequate number of high-quality formed samples is a requirement that cannot be

easily given in fragile or heavily weathered rocks [31,2,17][3].

For creating empirical equations, statistical methods such as simple and multiple regression approaches are widely employed [11,4,3,57] [56]. Several equations for the UCS prediction have been established in recent years, some of which are described in Table 1.

Today, soft computational methods have shown promising potential ability in engineering problems [79,40]. Soft computing is an emerging approach to computing that parallels the human mind's remarkable power to reason and learn in uncertain and imprecision [68]. Researchers have previously been drawn to modern UCS prediction approaches focused on probabilistic and soft computation strategies such as particle swarm optimization (PSO), support vector regression (SVR), genetic programming (GP), generalized feed forward neural network (GFFN), radial basis function (RBF), multiple linear regression (MLR),

\* Corresponding author.

E-mail addresses: [arsalan.mahmoodzadeh@uoh.edu.iq](mailto:arsalan.mahmoodzadeh@uoh.edu.iq) (A. Mahmoodzadeh), [mukhtar@lpu.edu.krd](mailto:mukhtar@lpu.edu.krd) (M. Mohammadi), [hawkar.ibrahim@su.edu.krd](mailto:hawkar.ibrahim@su.edu.krd) (H. Hashim Ibrahim), [sazan.abdulhamid@su.edu.krd](mailto:sazan.abdulhamid@su.edu.krd) (S. Nariman Abdulhamid), [sirwan.ghafoor@sput.edu.iq](mailto:sirwan.ghafoor@sput.edu.iq) (S. Ghafoor Salim), [hunar.hamaali@uoh.edu.iq](mailto:hunar.hamaali@uoh.edu.iq) (H. Farid Hama Ali), [mohammed.kamal@tiu.edu.iq](mailto:mohammed.kamal@tiu.edu.iq) (M. Kamal Majeed).

**Table 1**  
Some simple and multiple regression equations for predicting UCS.

References	Equation	Rock type
Tugrul and Zarif [69],	$UCS = 183 - 16.55n$	Granite
Palchik [59],	$UCS = 74.4 \exp(-0.04n)$	Sandstone
Alvarez Grima and Babuska [5],	$UCS = 0.386EH + 39.268\rho - 1.307n - 246.804$	Sandstone, limestone, dolomite, granite, and granodiorite
Meulenkamp & Alvarez Grima [42],	$UCS = 0.25EH + 18.14\rho - 0.75n - 15.47GS - 21.55RT$	Sandstone, limestone, dolomite, granite, and granodiorite
Lashkaripour [37],	$UCS = 10.1 \exp(-0.821n)$	Shale, claystone, and siltstone
Yilmaz and Sendir [70],	$UCS = \exp(0.818 + 0.059SH)$	Gypsum
Tsiambas and Sabatakis [71],	$UCS = 7.3 \text{ PLS}^{1.71}$	Limestone, sandstone, and marl
Gokceoglu and Zorlu [19],	$UCS = 0.0065V_p + 1.468PI + 4.094PLS + 2.418TS - 225$	Weak, fractured, and thin-bedded rocks
Yasar and Erdogan [80],	$UCS = 31.5V_p - 63.7$	Dolomite, marble, and limestone
Aydin and Basu [6],	$UCS = 1.4459 \exp(0.0706SH)$	Granitic rocks
Karakus and Tutmez [35],	$UCS = 0.89SH + 13.1PLS - 1.68V_p - 35.9$	Marble, limestone, and dacite
Tiryaki [73],	$UCS = 0.88 \rho^{2.24} SH^{0.22} CI^{0.89}$	Igneous and sedimentary rocks
Yilmaz and Yuksek [84],	$UCS = 0.48SH + 1.863PLS + 248WC + 7.972V_p - 23.859$	Gypsum
Yagiz [81],	$UCS = 0.0028^{2.584 SH}$	Travertine, limestone, dolomitic
Moradian and Behnia [88]	$UCS = 165.05 \exp(-4.452/V_p)$	limestone, and schist
Dehghan et al. [15],	$UCS = -595.303 - 442.363V_p + 45.338V_p^2 - 6.1n + 0.52n^2 + 28.314(I_{50}) - 4.06(I_{50})^2 + 115.822SH - 2.007SH^2$	Travertine
Yagiz [82],	$UCS = 29.63SD - 28.58$	Limestone, marble, and sandstone
Altindag [1],	$UCS = 5.734V_p + 10.876TS - 2.408PLS - 10.029$	Travertine, limestone, and dolomitic limestone
Nefeslioglu [58],	$UCS = 0.458 \exp(1.504V_p)$	Sedimentary rocks
Mishra and Basu [45],	$UCS = \exp(0.011BPI + 0.065PLS + 0.029SH + 0.00012V_p + 2.157)$	Claystone and mudstone
Kahraman [32],	$UCS = 12.5PLS$	Granite, schist, and sandstone
Karaman et al. [33],	$UCS = 24.301 + 4.874TS$	Pyroclastic rocks
Kahraman et al. [34],	$UCS = 0.047 \exp(0.065SD)$	Basalt and limestone
Madhubabu et al. [51],	$UCS = -2.572n + 23.665PLS + 41.654PR + 12.197\rho - 0.001V_p - 11.813$	Pyroclastic rocks
Jahed Armaghani et al. [30],	$UCS = -153.61n + 0.010V_p + 7.111(I_{50})$	Granite
Matin et al. [53],	$UCS = -120.912 - 2.036V_p + 31.064(I_{50})$	Travertine
Heidari et al. [25],	$UCS = 1.277SHN + 2.186BPI + 16.41(I_{50}) + 0.011V_p - 82.436$	Grainstone, wackestone-mudstone, boundstone, gypsum, and silty marl
Mahdiabadi & Khanlari [54],	$UCS = -6.479 + 3.425BPI + 0.639CPI + 7.889(I_{50})$	Mudstone
Celik [11],	$UCS = 29.3UW + 0.4V_p - 687.43$	Marble, dolomite, limestone, and travertine
	$UCS = 15.14UW + 2.88SHR - 446.3$	
	$UCS = -6.53L + 3.63V_p + 3.45SHR - 50.68$	

**Note:** n: Porosity; EH: Equotip hardness; ρ: Density; GS: Grain size; RT: Rock type; SH: Schmidt hammer number; V<sub>p</sub>: P-wave velocity; PLS: Point load strength; I<sub>(50)</sub>: Point load index; TS: Tensile strength; CI: Cone indenter hardness; WC: Water content; SD: Slake durability index; BPI: Block punch index; PR: Poisson's ratio; BPI: Block punch index; CPI: Cylinder punch index; UW: Unit weight; SHR: Schmidt hardness rebound number; L: Cubic sample sizes.

adaptive neuro-fuzzy inference systems (ANFIS), multi-layer perceptron (MLP), artificial neural networks (ANN), Sugeno fuzzy logic (SFL), imperialist competitive algorithm (ICA), Random Forest (RF), Mamdani fuzzy logic (MFL) [42,21][19][64][35][73][8,87][83][22][12][84] [65][15][13][85][44][60][45][46][48][86][9,14][28][74][49][75] [50][29][30][51][18][10,17][53][25][3,54][11].

Alvarez Grima and Babuska [5], have shown that the fuzzy model estimates the UCS more than by multiple regression analysis techniques. The UCS prediction for clay-bearing rocks, travertine, carbonate, schistose, sandstones using several regression models and ANN are made by numerous researchers such as Meulenkamp and Alveraz Grima [42], Singh et al. [61], Dehghan et al. [15], Cevik et al. [13], and Ceryan et al. [14]. They found out that the ANN-based models have more reliable forecasts than conventional statistical techniques. In calculating UCS using MR, ANN and ANFIS approach subjected to three separate models and five datasets, Gultekin et al. [20], demonstrated greater predictability in ANFIS. Furthermore, a study shows a result comparison of predicted UCS from various soft computing approaches in which ANFIS shows a greater efficiency than others[43,62][3]. Singh et al. [63], demonstrated the model of ANFIS and the generalized models of neural network regression and states far more accuracy in network prediction of the UCS than ANFIS. The AI model, integrated with the metaheuristic optimization algorithm, was also confirmed to be even more predictable [24,28]. Increasing the UCS predictability level can be done using particle swarm optimization with the ANN model Momeni et al. [50], Taghavifar et al. [72], and Jahed Armaghani et al. [29], show that the hybrid ICA-ANN, an Optimisation ANN by ICA, is more developed in predicting and accuracy than the conventional ANN technique. In their work, Ferentinou and Fakir [17], developed an ANN framework for estimating the UCS of certain sedimentary and igneous rocks and demonstrated that the model established is accurate and could be used as an alternate indirect approach to the UCS estimation. In their study, Matin et al. [53], used the RF approach to the UCS prediction, noting that the implementation of a non-linear interdependence approximation between variable selection parameters as well as a non-parametric predictive model using soft computing methods such as RF could potentially be used as a reliable and accurate UCS evaluation and estimation technique. Asheghi et al. [3], introduced ICA and GFFN (ICA-GFFN) models to forecast UCS. They concluded that their model could be used successfully for UCS prediction purposes as a reliable and feasible method. Through the sensitivity analyzes, rock class and P-wave velocity (V<sub>p</sub>) have been the least and most influential variables in the UCS prediction.

Such studies all have shown more precision in using soft computing methods to forecast UCS than conventional statistical models. The fundamental drawback to these approaches is that, in most situations, the interaction between inputs and results does not provide a deterministic mathematical pattern. This indicates that such approaches are not as straightforward and understandable as regression-based models and empirical formulas, that's why they are called "black box" [18].

Although many studies have been done on predicting the UCS parameter using the different computational methods, other methods have not yet been used for this purpose or have rarely been used. Therefore, it is necessary to carefully consider the predictability of other computational methods in order to predict the UCS parameter. For this purpose, in this study, six computational methods of long short term memory (LSTM), deep neural networks (DNN), K-nearest neighbor (KNN), Gaussian process regression (GPR), support vector regression (SVR), and decision tree (DT) have been utilized to predict the UCS parameter by applying 170 data sets of different rock types including porosity (n), Schmidt hammer (SH), P-wave velocity (V<sub>p</sub>), and point load index (I<sub>(50)</sub>). All the data sets were acquired from almost all quarry locations of Iran. Before modeling, all the parameters were normalized to reduce the range of input and output parameters' variations. To assess the performance ability of the applied methods, the 5-fold cross-validation (CV) was considered. Finally, for the prediction results of

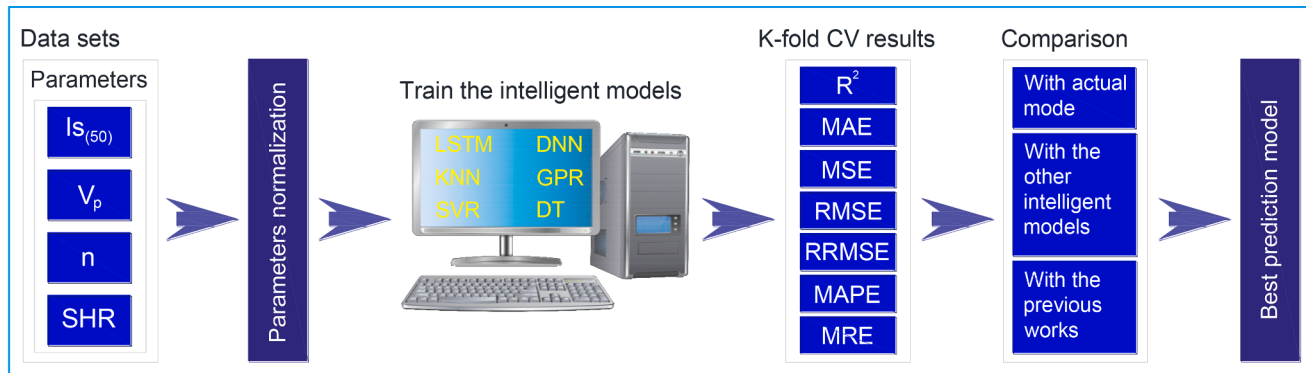


**Fig. 1.** A summary of this article steps in a schematically way.

each model, different evaluation criteria of the coefficient of determination ( $R^2$ ), mean absolute error (MAE), mean square error (MSE), root mean square error (RMSE), relative RMSE (RRMSE), mean absolute percentage error (MAPE), and mean relative error (MRE), were evaluated. In the next step, a comparison was made between the results of each model with the other models, with the actual mode, and with the previous works in the field. Lastly, the best intelligent model for UCS prediction was specified and suggested for future studies' UCS prediction. A summary of this article's steps is presented in Fig. 1, schematically.

The rest of the paper is structured as follows: In section 2, a discussion regarding the database used in this study is provided. In section 3, the different methods to analyze the intelligent models' results are introduced. In section 4, the intelligent models applied in this study are described in detail and the prediction results are analyzed. A comparison is made in section 5 between each intelligent model's prediction results with the other models and previous works in the field from 1999 to 2019. Discussion and conclusions are described in section 6. Fig. 1 shows a summary of this article's steps, schematically.

## Database

Based on the previous studies done on the UCS prediction using intelligence methods (see Table 1), four effective rock properties on the UCS including porosity (n), Schmidt hammer number (SHN), P-wave velocity ( $V_p$ ), and point load index ( $Is_{(50)}$ ) were considered in this article. At all, 170 data sets were acquired from almost all of Iran's quarry locations (Table 2). A series of laboratory tests obtained the database on Claystone, Granite, Schist, Sandstone, Travertine, Limestone, Slate, Dolomite and Marl samples. A summary of the database used is presented in Table 3. Compared to many previous research types, a more comprehensive range of the database has been considered in this study.

## Results analysis methods

Seven statistical evaluation criteria are used to assess the performances of the intelligent methods on the prediction results. These criteria are the coefficient of determination ( $R^2$ ), mean absolute error (MAE), mean square error (MSE), root mean square error (RMSE), relative RMSE (RRMSE), mean absolute percentage error (MAPE), and mean relative error (MRE), respectively, given by Eqs. 1–7.

$$R^2 = \left( \frac{\sum_{i=1}^n (f(x_i) - f_{-}(x))(f^{*}(x_i) - f^{*}_{-}(x))}{\sqrt{\sum_{i=1}^n (f(x_i) - f_{-}(x))^2 \sum_{i=1}^n (f^{*}(x_i) - f^{*}_{-}(x))^2}} \right)^2 \quad (1)$$

$$MAE = \left( \frac{1}{n} \sum_{i=1}^n |f(x_i) - f^{*}(x_i)| \right) \quad (2)$$

$$MSE = \frac{1}{n} \sum_{i=1}^n (f(x_i) - f^{*}(x_i))^2 \quad (3)$$

$$RMSE = \sqrt{\left( \frac{1}{n} \sum_{i=1}^n (f(x_i) - f^{*}(x_i))^2 \right)} \quad (4)$$

$$RRMSE = \sqrt{\left( \frac{1}{n} \sum_{i=1}^n \left( \frac{f(x_i) - f^{*}(x_i)}{f_{-}(x_i)} \right)^2 \right)} \quad (5)$$

$$MAPE = \frac{100\%}{n} \sum_{i=1}^n \left| \frac{f(x_i) - f^{*}(x_i)}{f_{-}(x_i)} \right| \quad (6)$$

$$MRE = \left( \frac{1}{n} \sum_{i=1}^n \frac{|f(x_i) - f^{*}(x_i)|}{|f_{-}(x_i)|} \right) \quad (7)$$

where  $f(x)$  is the actual value and  $f^{*}(x)$  is the predicted value,  $f_{-}(x)$  and  $f^{*}_{-}(x)$  are the means of actual and predicted values, and  $n$  is the number of data sets.

## UCS prediction using intelligent methods

MATLAB software 2018 was used for GPR, SVR, DT and LR modeling in this study. The implementation environment for LSTM, DNN, and KNN algorithm was Anaconda version 3.6. Anaconda is a *meta*-package that includes all of the Python packages. To identify the UCS's best predictive model, these six predictive models were applied. All parameters were normalized in [-1, 1] intervals before modeling to minimize input and output differences. However, the data's normalization was not sufficient and the findings were unfavorable because of an excessive dispersal of data. So, K-fold cross-validation (CV) was considered in this study ( $K = 5$ ) to assess prediction results. For K-fold cross-validation, the initial sample is uniformly subdivided into  $K$  equal-sized subsamples. As validation data for model testing, a single subsample of the  $K$  subsamples is retained, and the  $K - 1$  subsamples remain used as training data. Since each observation is used only once for the validation process and all observations are used for validation and training, this approach became more advantageous than the over repeated random sub-sampling method.

### LSTM

Deep learning or deep structured learning can be described as a special form of multi-layered neural networks. Here, the information from previous events is better preserved by these networks than by conventional neural networks. A recurrent neural network (RNN) is a type of neural network with network combinations in a loop [52,55]. Through these loops in the networks, information persistence will occur. That network in the loop takes inputs and information from the previous network, executes the specified procedure, produces an output, and

**Table 2**

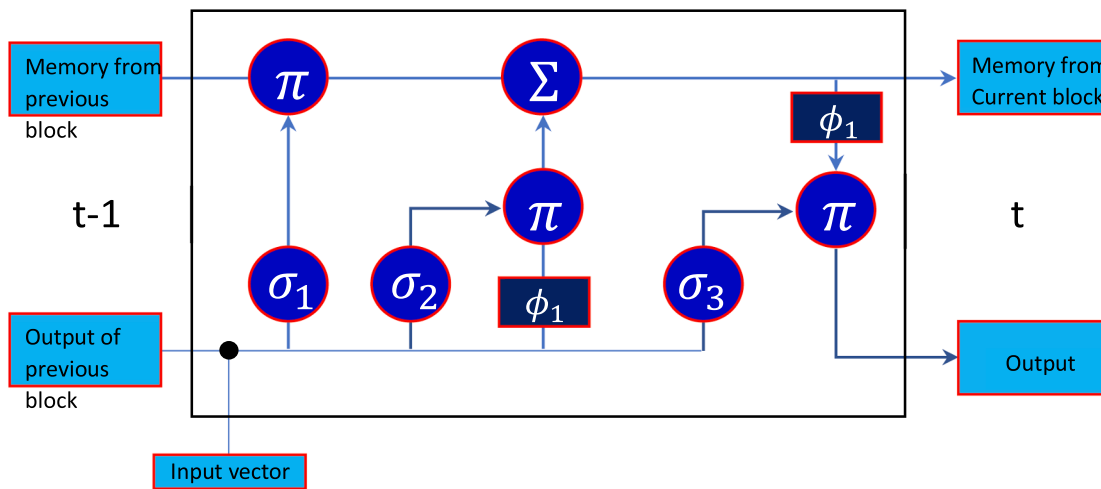
Results of laboratory tests conducted in this study.

No.	n [%]	SHR	Vp [m/ s]	Is <sub>(50)</sub> [Mpa]	UCS [Mpa]	*Rock type	No.	n [%]	SHR	Vp [m/ s]	Is <sub>(50)</sub> [Mpa]	UCS [Mpa]	*Rock type	No.	n [%]	SHR	Vp [m/ s]	Is <sub>(50)</sub> [Mpa]	UCS [Mpa]	*Rock type
1	0.44	38.00	6450	2.87	132.21	Li	58	0.870	32.40	6112	7.23	50.340	Sa	115	0.40	46.30	5993	3.930	120.30	Li
2	0.15	52.00	6148	3.89	166.30	Sa	59	0.320	54.00	6790	5.59	135.09	Li	116	0.25	52.55	6074	4.490	150.32	Li
3	0.23	46.00	5920	1.82	215.21	Sa	60	0.370	52.00	6503	3.12	170.94	Gr	117	0.40	52.17	5172	4.030	100.00	Cl
4	0.47	44.00	4780	2.40	120.90	Gr	61	0.330	56.00	5040	4.65	92.320	Sa	118	0.42	43.46	5820	3.170	145.00	Li
5	0.15	57.00	6102	4.56	143.21	Li	62	0.220	49.00	6430	2.99	195.00	Sa	119	0.50	37.76	5116	1.520	170.90	Sa
6	0.40	56.00	5020	3.01	77.300	Sc	63	0.470	51.00	5715	4.88	111.00	Sc	120	0.54	45.36	5675	3.070	128.00	Sc
7	0.20	52.00	6910	7.10	114.54	Sa	64	0.570	40.00	4233	1.21	95.870	Cl	121	0.53	43.46	5882	3.270	125.00	Li
8	0.42	47.00	5025	1.73	130.33	Sa	65	0.250	56.70	5491	6.93	125.00	Li	122	0.20	58.59	6250	7.420	135.21	Sa
9	0.37	49.00	4910	3.79	103.23	Gr	66	0.280	60.48	5566	6.92	117.45	Do	123	0.42	41.25	5850	3.470	137.00	Li
10	0.40	47.00	4670	3.34	92.120	Li	67	0.280	45.36	6188	3.58	155.36	Sa	124	0.35	54.18	6145	4.850	124.30	Do
11	0.41	45.00	6190	3.14	150.05	Sa	68	0.320	35.67	6024	3.24	114.23	Sa	125	0.50	33.95	5321	1.150	174.20	Li
12	0.40	48.00	4568	2.45	81.050	Cl	69	0.700	44.18	6190	8.90	83.430	Sl	126	0.29	46.30	6145	6.060	115.89	Sc
13	0.43	57.00	5785	1.98	112.32	Li	70	1.780	42.00	5052	8.78	55.980	Cl	127	0.31	43.08	6043	4.250	140.00	Do
14	0.15	57.00	7002	4.97	163.30	Li	71	14.30	30.98	4188	2.92	37.670	Ma	128	0.24	55.76	6179	6.630	132.62	Li
15	0.43	45.00	7310	1.45	209.00	Sa	72	0.250	45.00	5950	3.12	175.43	Sa	129	0.57	50.00	4490	1.670	52.100	Ma
16	0.37	49.00	6635	2.02	200.23	Li	73	0.420	52.00	6848	3.56	152.30	Li	130	0.55	42.00	4230	1.310	87.540	Cl
17	0.44	50.00	7608	2.51	185.21	Sa	74	0.490	49.00	5270	3.89	99.000	Tr	131	0.48	39.00	4003	1.020	112.93	Li
18	0.40	53.00	6080	3.23	149.05	Sa	75	3.840	55.95	4441	8.38	80.000	Sc	132	0.50	46.00	4480	1.330	90.020	Tr
19	0.42	58.00	6620	3.21	155.90	Sa	76	8.350	49.14	4219	6.21	60.550	Sl	133	0.51	48.00	4108	1.340	59.320	Cl
20	0.39	46.00	4432	2.89	83.950	Sc	77	6.100	31.47	5521	7.79	44.780	Li	134	0.47	46.00	5250	2.780	132.02	Gr
21	0.45	50.00	4922	2.44	84.090	Tr	78	1.730	42.29	5875	3.63	30.560	Ma	135	0.45	48.00	4876	3.230	95.340	Li
22	0.43	54.00	5380	3.49	95.000	Gr	79	3.100	31.31	5445	6.56	35.460	Ma	136	0.50	37.00	5463	4.230	95.320	Sc
23	0.19	57.00	7433	5.23	155.67	Sa	80	2.890	51.79	4672	6.75	58.980	Sl	137	0.48	44.00	5520	4.020	110.82	Li
24	0.39	46.00	5545	4.11	122.38	Li	81	14.50	30.89	2725	1.98	17.330	Li	138	0.50	53.00	5109	3.670	80.320	Sc
25	0.44	42.00	4955	3.21	120.02	Tr	82	15.30	25.89	2786	1.33	12.010	Cl	139	0.51	47.00	4659	2.890	77.680	Sc
26	0.10	60.00	7850	6.12	155.32	Gr	83	3.080	58.59	4624	9.08	80.870	Sc	140	3.35	27.42	5660	3.000	23.120	Ma
27	0.22	49.00	5988	4.92	140.43	Li	84	10.90	41.09	3169	3.70	39.240	Li	141	8.14	30.13	5090	3.630	37.890	Sc
28	0.36	48.00	4615	3.34	92.100	Cl	85	4.520	54.18	4522	9.59	89.540	Cl	142	2.24	25.75	5810	3.100	28.330	Cl
29	0.12	61.00	7943	6.54	154.30	Sc	86	0.390	47.00	5506	2.31	155.00	Sa	143	9.76	27.38	5350	3.390	43.460	Si
30	0.11	56.00	5980	5.86	140.32	Li	87	0.160	51.00	5217	6.22	125.00	Sa	144	4.50	26.00	5590	3.160	24.320	Ma
31	0.28	59.00	6005	4.78	120.00	Gr	88	0.460	50.00	5345	1.93	125.00	Sa	145	8.32	29.75	5250	4.010	37.650	Si
32	0.30	53.00	6125	2.25	176.40	Sa	89	0.360	43.00	4320	1.41	116.00	Li	146	9.45	29.13	5390	3.740	41.510	Cl
33	0.18	51.00	6555	3.13	190.32	Gr	90	9.350	27.38	5380	2.86	37.480	Sa	147	9.22	26.88	5230	3.080	35.670	Sc
34	0.29	45.00	6120	4.15	144.00	Tr	91	9.640	27.63	4820	2.54	38.190	Ma	148	7.42	28.00	5400	3.600	32.350	Ma
35	0.18	58.00	6895	5.29	154.30	Li	92	2.930	26.75	5670	2.26	25.670	Cl	149	3.95	26.50	5730	3.020	24.180	Sc
36	0.19	56.00	6615	5.38	148.00	Sa	93	9.510	30.50	5050	2.63	32.950	Ma	150	6.38	29.63	5100	3.360	35.670	Sc
37	0.20	58.00	6709	4.33	160.00	Sa	94	8.980	27.63	5090	3.32	38.340	Li	151	9.28	27.50	5520	3.300	40.130	Ma
38	0.28	51.00	6301	5.02	141.70	Sc	95	3.490	27.38	5790	3.02	25.370	Ma	152	3.97	27.38	5490	3.520	25.980	Ma
39	0.30	57.00	6150	3.22	143.90	Gr	96	0.150	66.51	6047	9.92	138.00	Sa	153	4.89	26.63	5420	2.910	25.120	Ma
40	0.51	40.00	2823	1.02	35.000	Ma	97	0.350	55.76	5428	7.85	115.00	Gr	154	3.78	30.30	5510	3.060	23.110	Cl
41	0.56	37.00	3065	0.91	42.000	Ma	98	14.75	42.51	2830	2.57	27.610	Ma	155	0.97	25.63	5450	3.890	29.050	Cl
42	0.54	43.00	4635	1.39	113.90	Do	99	8.720	51.03	3474	4.36	66.900	Sl	156	7.99	28.63	5020	3.320	35.680	Ma
43	0.06	65.38	6214	11.3	158.02	Sa	100	0.470	35.52	6419	2.12	140.30	Li	157	6.66	29.88	4840	2.610	30.130	Ma
44	0.14	61.80	5729	9.23	144.20	Tr	101	4.820	36.60	5154	6.89	45.000	Cl	158	8.93	29.25	5400	3.260	38.980	Ma
45	0.22	57.64	6030	9.72	132.45	Li	102	3.830	29.31	4865	1.00	32.100	Ma	159	9.13	26.25	5190	3.870	39.130	Cl
46	0.40	52.92	5384	5.66	112.40	Do	103	9.740	27.02	4149	5.44	51.200	Sa	160	9.29	28.25	5130	3.170	35.660	Ma
47	0.48	52.00	5643	2.75	122.00	Sa	104	1.540	34.96	5980	0.86	69.700	Sl	161	10.2	28.88	5090	2.920	37.430	Cl
48	0.25	58.00	6080	5.21	130.20	Do	105	0.800	44.09	6768	5.90	52.100	Cl	162	0.28	55.38	5865	8.350	122.21	Li
49	0.31	55.00	4978	3.72	93.800	Sc	106	0.800	34.21	6052	7.03	61.870	Sl	163	0.21	65.38	5836	10.85	135.87	Sa
50	0.52	38.00	3268	0.89	48.080	Ma	107	10.10	25.46	2977	2.24	35.610	Ma	164	0.15	64.43	5945	10.02	132.21	Sa
51	0.47	51.00	4530	2.43	62.100	Ma	108	8.390	51.22	3935	5.80	69.200	Tr	165	0.18	65.57	5905	11.73	145.87	Gr
52	2.11	26.13	5540	2.73	30.600	Sl	109	12.14	35.86	3389	4.50	40.020	Cl	166	0.12	67.07	6250	14.13	180.41	Li
53	3.48	27.63	5670	2.98	24.320	Cl	110	10.69	30.32	2795	1.25	18.390	Ma	167	0.19	60.48	6030	10.63	148.34	Sa
54	0.46	46.30	5445	3.48	125.00	Li	111	14.67	33.38	2985	2.99	23.450	Sl	168	0.22	58.59	5753	8.490	134.76	Sa
55	0.50	31.66	5685	2.45	100.09	Sa	112	8.440	52.29	3508	4.47	70.830	Li	169	0.31	58.59	5422	7.870	102.32	Li
56	0.43	49.14	5882	2.96	151.30	Sa	113	7.230	46.30	3658	3.31	44.000	Cl	170						

**Table 3**

A brief review of the datasets used.

	n [%]	SHR	V <sub>p</sub> [m/s]	I <sub>S(50)</sub> [Mpa]	UCS [Mpa]
count	170.000000	170.000000	170.000000	170.000000	170.000000
mean	2.795588	44.406824	5368.542529	4.258882	96.039000
std	4.128324	11.452733	1026.920912	2.499021	51.112274
min	0.060000	25.460000	2725.000000	0.000000	12.010000
25%	0.310000	33.522500	4884.500000	2.800000	41.632500
50%	0.470000	46.000000	5490.500000	3.430000	99.500000
75%	3.837500	53.000000	6030.000000	5.357500	136.717500
max	16.800000	67.070000	7943.000000	14.130000	215.210000

**Fig.2.** LSTM Repeating Module [36].,

fowards the information to the next network. Some applications need recent information only, whereas others may request more from the past. A lag in learning happens in recurrent neural networks when the gap between the required prior information and the point of requirement increases significantly. But fortunately, Long Short-Term Memory (LSTM) Networks, which are a particular form of RNN [26], capable of learning such scenarios. These networks are explicitly designed to avoid the problem of recurrent networks' long-term dependency.

Long time information remembering is an important feature of LSTM. LSTMs are a natural choice because the model's accuracy is almost always dependent on the amount of previous information. The standard LSTM module, known as the repeated module, has four neural network layers interacting especially. As seen in Fig. 2. The module is composed of three activation function gates which are  $\sigma_1$ ,  $\sigma_2$ , and  $\sigma_3$  and it owns two activation functions regarding the output, which are  $\Phi_1$  and  $\Phi_2$  as clearly shown in Fig. 2. The  $\pi$  and  $\Sigma$  symbols are representing the element-wise multiplication and addition, respectively. A symbol ( $\bullet$ ) bullet represents the concatenation operation. The fundamental component of LSTM is the cell state, in which a line comes from the previous block memory ( $S_{t-1}$ ) to the current block memory ( $S_t$ ). Afterward, the flow of information straight down the line is allowed. The amount of previous information that should be flowed is decided by the network, done by the first layer ( $\sigma_1$ ). Eq. (8) below shows the operation performed by this layer [36].

$$c_{ft} = \sigma_1(W_{cf}\hat{A} \cdot [O_{t-1}, x_t] + b_{cf}) \quad (8)$$

$$I_t = \sigma_2(WI\hat{A} \cdot [O_{t-1}, x_t] + bI) \quad (9)$$

$$\tilde{S}_t = \tanh(WS\hat{A} \cdot [O_{t-1}, x_t] + bS) \quad (10)$$

$$S_t = (c_{ft} \times S_{t-1}) + (I_t \times \tilde{S}_t) \quad (11)$$

Here, two network layers affect the process of storing new

information in the cell state. A sigmoid layer ( $\sigma_2$ ) which determines the ( $I_t$ ) value to be updated, see Eq. (9) and  $\Phi_1$  tanh layer, which establishes a new candidate value ( $\tilde{S}_t$ ) as seen in Eq. (10). The combination of both to be added in the state. The cell state is finally changed with Eq. (11).

Here we are creating training data from the dataset we have. In the script below, we create an LSTM model of four layers of 32 neurons with a single neuron output and ReLU activation functions, which stands for rectified linear unit. The below model has parameter return\_sequences set to true, which means the output of each neuron's hidden state is used as an input to the next LSTM layer. The model uses Nadam Optimizer. From callbacks, ModelCheckpoint is imported, which saves the Keras model or model weights at some frequency. The callback is an object that can perform actions at various stages of training (e.g. at the start or end of an epoch, before or after a single batch, etc.). A sequential model is then created, which is a linear stack of layers that accepts a list of layer instances to its constructor. An input\_shape is passed as an argument to the first layer, which is a shape tuple. The input shape is (1,4) since the data has one time-step with four features. The batch\_size is 10, which means we train the model, iterating on the data in batches of 10 samples and it continues for 100 epochs.

```

Model = Sequential()
model.add(LSTM(32, activation = 'relu', return_sequences = True,
input_shape = (1,4)))
model..add(Dropout(0.2))
model.add(LSTM(32, activation = 'relu', return_sequences = True))
model..add(Dropout(0.2))
model.add(LSTM(32, activation = 'relu', return_sequences = True))
model..add(Dropout(0.2))
model.add(LSTM(32, activation = 'relu'))
model..add(Dropout(0.2))
model.add(Dense(1, input_shape = (X_test.shape [1,]), activation =
'relu', kernel_initializer = 'lecun_uniform'))
checkpoint = ModelCheckpoint('model_train.h53', verbose = 1,
```

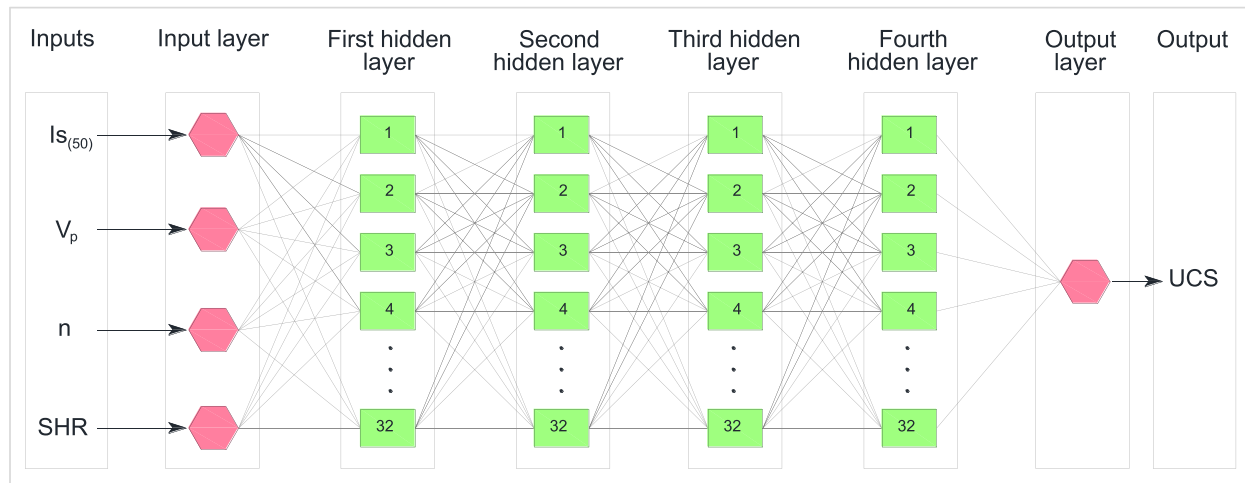


Fig. 3. The LSTM model network used in this study.

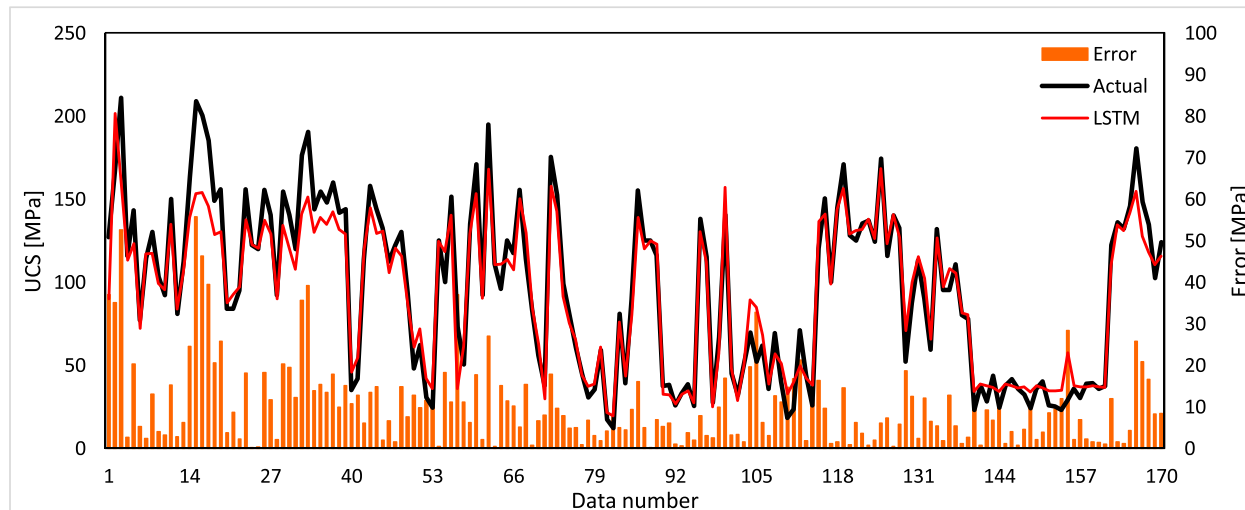


Fig. 4. UCS prediction results of the LSTM model.

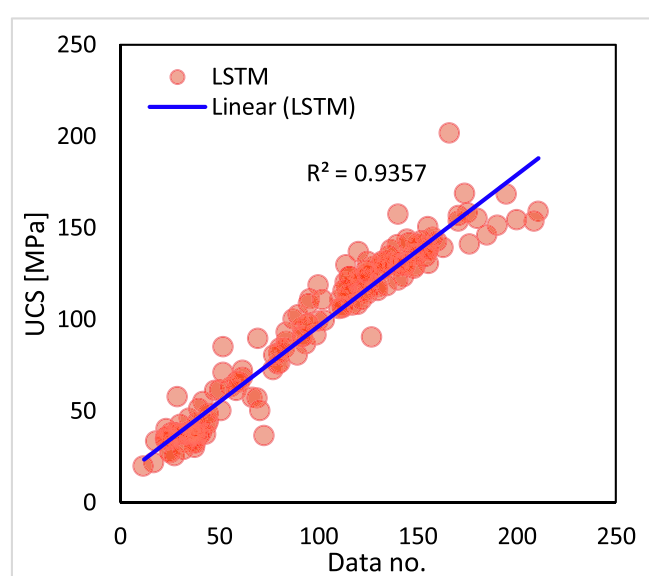


Fig. 5. Prediction performance of LSTM method on UCS prediction.

```

monitor = 'val_loss', save_best_only = True, mode = 'auto')
model.compile(optimizer = 'Nadam', loss = 'mean_squared_error',
metrics = ['accuracy'])
model.fit(X_train, y_train, batch_size = 10, epochs = 100,
validation_split = 0, callbacks = [checkpoint], verbose = 1)

```

The LSTM model network is shown in Fig. 3, schematically.

The LSTM model results are presented in Figs. 4 and 5. In Fig. 4, the LSTM prediction results are compared with the actual results and the prediction errors are shown. The  $R^2$  value is obtained by 0.9357, which confirms the LSTM model's high ability in the UCS prediction. The results of seven statistical methods applied in this study are presented in Table 4. According to these results, a good accuracy can be seen in the LSTM results. Therefore, considering the database applied in this study, the LSTM model is an effective USC prediction method.

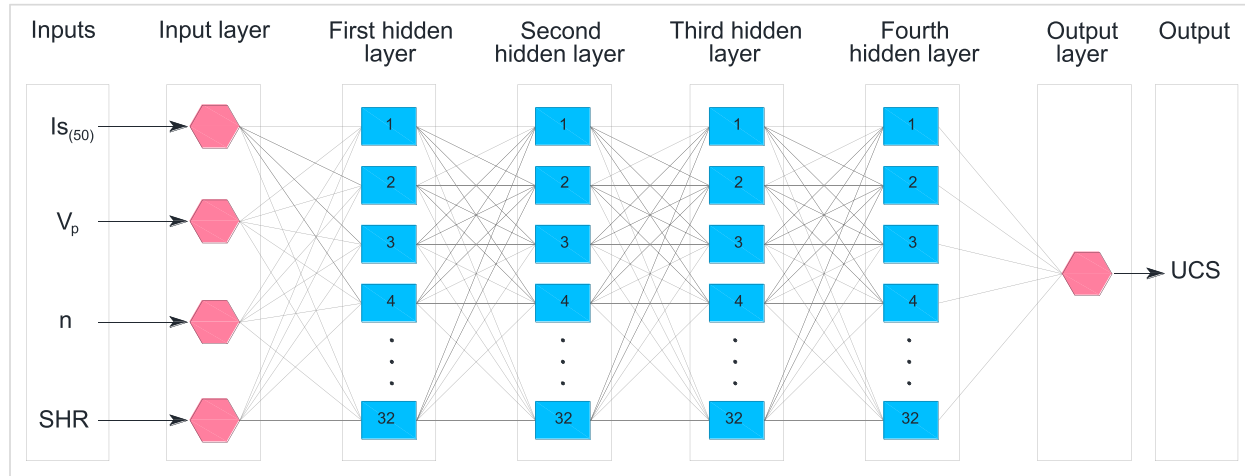
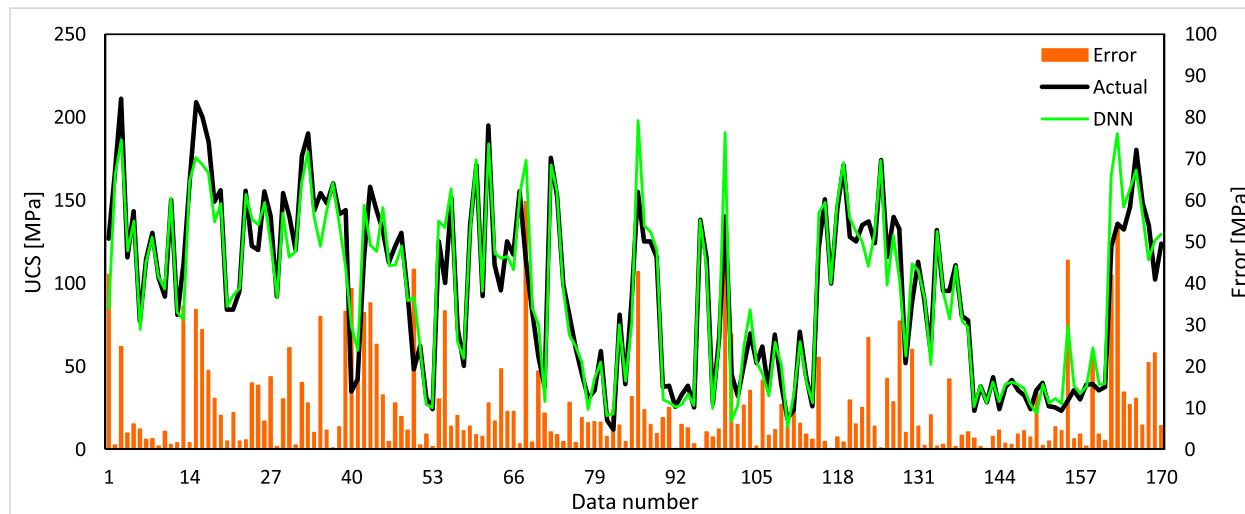
#### DNN

DNN (Deep Neural Network) is a feed-forward neural network with more than one layer of hidden units between its inputs and outputs. There are the input layers; after that, mid-layers come, hidden layers, and then the output layer follows. The network is ultimately connected to the neighboring layers, which start with input, then hidden layers, and the output layer. Its feed-forward, which means there is no

**Table 4**

Evaluation criteria results of the LSTM model.

R <sup>2</sup>	MAE	MSE	RMSE	RRMSE	MAPE [%]	MRE
0.9357	2.18E-01	8.052941176	2.837770459	0.022344649	0.171375637	0.001713756

**Fig. 6.** The DNN model network applied in this study.**Fig. 7.** UCS prediction results of the DNN model.

backward feeding and the links between the layers are one way, which is in the forward direction. DNN is especially suitable for analyzing data input because of its potential to detect patterns and learn useful features from raw input data without extensive feature engineering, data pre-processing, or hand-crafted rules. Furthermore, its performance even increases with the increase of the training data [27]. DNNs have a wide variety of uses, text generation, computer vision tasks and automated translation are the earliest uses of DNN [66].

As in code presented below and as the network in Fig. 6, the DNN model considered for this study contains six layers where first layer contains four neurons, second, third, fourth, and fifth layers contain 32 neurons, and the last dense layer, which also acts as the result layer, contains 1 neuron.

Model = Sequential()

```
model.add(Dense(32, input_shape = (X_test.shape [1],), activation = 
'relu', kernel_initializer = 'lecun_uniform'))
model.add(Dense(32, activation = 'relu', return_sequences = True))
```

```
model.add(Dense(32, activation = 'relu', return_sequences = True))
model.add(Dense(32, activation = 'relu'))
model.add(Dense(1, input_shape = (X_test.shape [1],), activation = 
'relu', kernel_initializer = 'lecun_uniform'))
checkpoint = ModelCheckpoint('model_train.h53', verbose = 1, monitor = 'val_loss', save_best_only = True, mode = 'auto')
model.compile(optimizer = 'Nadam', loss = 'mean_squared_error', metrics = ['accuracy'])
model.fit(X_train, y_train, batch_size = 10, epochs = 100, validation_split = 0, callbacks = [checkpoint], verbose = 1)
```

The UCS prediction results of the DNN model are shown in Figs. 7 and 8. Comparing to the actual results, the DNN has presented accurate predictions. The other statistical indices results presented in Table 5, also mention to the high accuracy in the DNN predictions.

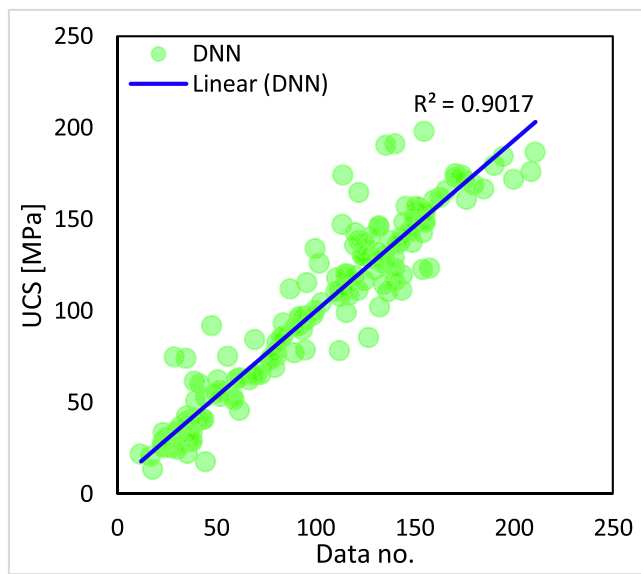


**Fig. 8.** Prediction performance of DNN method on UCS prediction.

#### KNN

KNN is one of the machine learning techniques that is based on supervised learning. KNN owns two types, KNN classification and KNN regression. KNN classification is utilized for classifying the training dataset into a set of classes based on similarities between the data. The new data is classified to the nearest classes of the data. The KNN regression is used to expect a constant value by calculating the average of the numbers of the K nearest neighbors. In other words, KNN regression is based on feature similarity to predict the value of new data points. The value is assigned to the new data point according to how closely the point looks like the training set, which already exists. Besides the importance of KNN, a renowned concern exists for KNN in general, population size. The extensive data size can slow down the execution speed and occupy a significant memory [67]. Nevertheless, it is not a big concern in this study since the used dataset is not that large for the

KNN method.

The simple mathematical implementation of KNN regression is based on calculating the average of the K nearest neighbors' target number. At least three distance functions could be used in simple implementation in KNN regression: Euclidean Distance Function, illustrated in Eq. (12), Manhattan Distance Function, which is illustrated in Eq. (13), and Minkowski Distance Function, which is illustrated in Eq. (14).

In the KNN model applied in this study, 1 neighbor ( $K = 1$ ) is considered.

$$\text{EuclideanDistanceFunction} = \sqrt{\sum_{i=1}^k (x_i - y_i)^2} \quad (12)$$

$$\text{ManhattanDistanceFunction} = \sum_{i=1}^k |x_i - y_i| \quad (13)$$

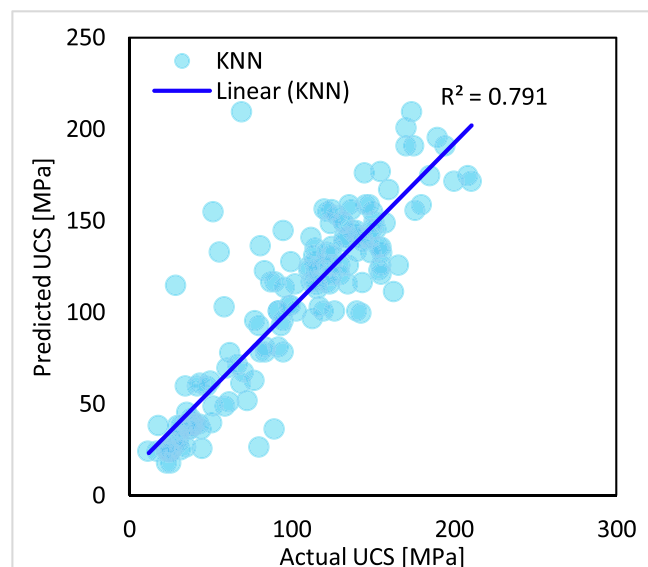


**Fig. 10.** Prediction performance of KNN method on UCS prediction.

**Table 5**

Evaluation criteria results of the DNN model.

$R^2$	MAE	MSE	RMSE	RRMSE	MAPE [%]	MRE
0.9017	2.47E-01	10.37647059	3.221252953	0.025364196	0.194534507	0.001945345

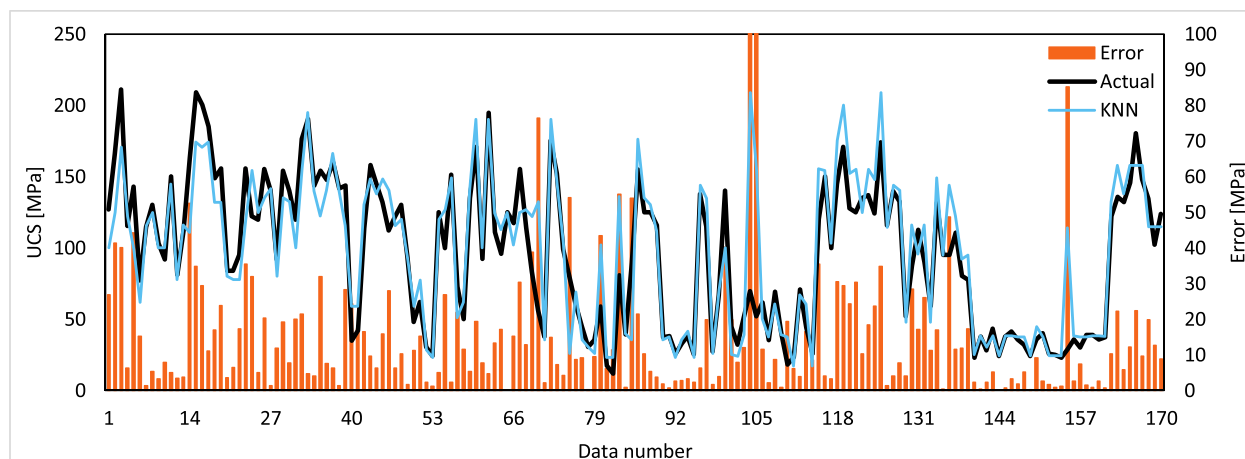


**Fig. 9.** UCS prediction results of the KNN model.

**Table 6**  
Evaluation criteria results of the KNN model.

R <sup>2</sup>	MAE	MSE	RMSE	RRMSE	MAPE [%]	MRE
0.7910	1.58E-01	4.259694706	2.063902785	0.016251203	0.124641038	0.00124641

**Table 7**  
An overview of the GPR model parameters.

Parameter	Value or type
KernelFunction (Form of the covariance function)	'Matern 5/2'
BasisFunction (Explicit basis in the GPR model)	'Constant'
Beta (Initial value of the coefficients for the explicit basis)	148.6882
Sigma (Initial value for the noise standard deviation of the Gaussian process model)	4.9467
FitMethod (Method to estimate parameters of the GPR model)	Exact Gaussian process regression

$$\text{MinkowskiDistanceFunction} = \left\{ \sum_{i=1}^k (|x_i - y_i|)^q \right\}^{1/q} \quad (14)$$

The UCS prediction results by the KNN model are shown in Fig. 9 nad 10. Looking at the error values in Fig. 9 and the R<sup>2</sup> of 0.791 in Fig. 10, the accuracy of the KNN model is not bad. The other statistical evaluation results for the KNN model are also presented in Table 6. However, it can not be said that this method has a high accuracy in in the UCS forecasting.

#### GPR

Gaussian processes (GP) are significant probabilistic techniques used in artificial intelligence [23]. Besides the GP's capabilities for classification, in another form, it is also used for regression, that named Gaussian process regression (GPR). GPR is a non-parametric kernel-based and supervised learning algorithm based on Bayesian non-linear regression [76]. It could be used for regressing values for both exploitation and exploration of unknown functions. Furthermore, the working mechanism is like. It utilizes probability distribution over all the possibilities using simple matrix manipulation. A simple linear regression model could be illustrated as in Eq. (15).

$$t^{(i)} = \alpha + \sum_{u=1}^p x_u^{(i)} \beta_{u+\epsilon^{(i)}} \quad (15)$$

Where t<sup>1</sup>, t<sup>2</sup>, ...etc., are the target values,  $\alpha$  and  $\beta$  are unknown,  $x^1$ ,  $x^2$ , ...etc., are set of cases with fixed inputs and  $\epsilon^{(i)}$  is the Gaussian noise

for case (i), which is assumed to be independent of a case to another.

GPR can work effectively as a useful technique for conducting inference passively such as explaining a dataset as excellent as possible, and permitting to predict future data based on the explanations, and also working actively like training the model to learn through selecting the input data to produce the highest possible output points [77].

The value and type of the GPR model parameters considered in this study are presented in Table 7.

The UCS results of the GPR model are shown in Fig. 11. Looking at Fig. 11, the error values indicate that the difference between the predicted results and the actual mode is negligible. The R<sup>2</sup> value of 0.9955 in Fig. 12, show the good prediction performance of the GPR model. All the other statistical indices in Table 8, proof the applicability of the GPR model in the UCS prediction considering the database applied in this study.

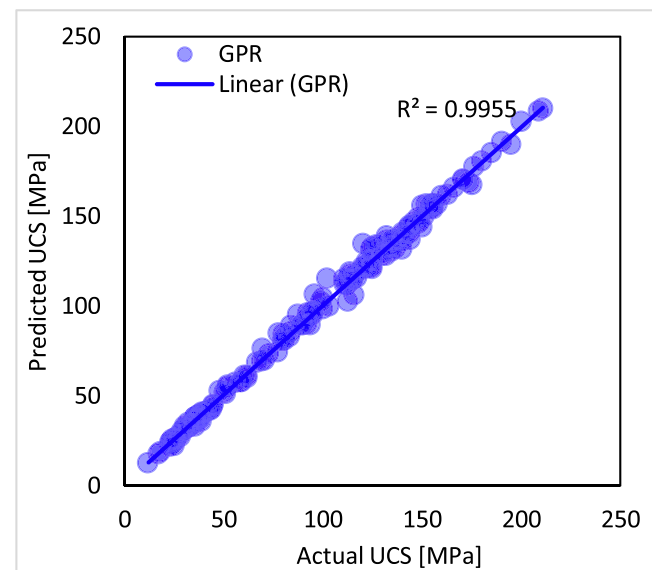


Fig. 12. Prediction performance of GPR method on UCS prediction.

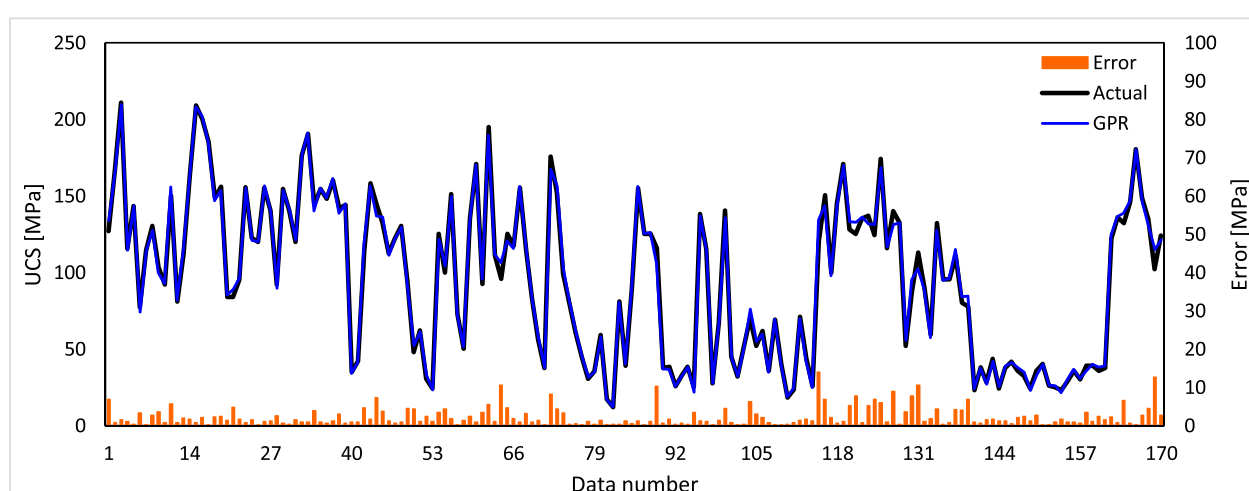


Fig. 11. UCS prediction results of the GPR model.

**Table 8**

Evaluation criteria results of the GPR model.

R <sup>2</sup>	MAE	MSE	RMSE	RRMSE	MAPE [%]	MRE
0.9955	4.00E-02	0.272160024	0.521689585	0.004107792	0.031505327	0.000315053

**Table 9**

An overview of the SVR model parameters.

Parameter	Value or type
Kernel Function	'Medium Gaussian'
Epsilon (Half the width of epsilon-insensitive band)	1
Solver (Optimization routine)	'SMO'
Bias	84.1285

### SVR

Support Vector Regression (SVR) maintains all the prevalent algorithm features named Support Vector Machine (SVM). The model is produced by SVM classification. As a result, SVM's principles for classification are similarly used for SVR. However, few minor differences enable the algorithm to be used as an effective technique for estimation of real-value functions. SVR permits the flexibilities to explain how much error is tolerable and it finds a suitable line or the hyperplane in higher dimensions for fitting with the data. Furthermore, it is characterized by utilizing the sparse solution, kernels, and Vapnik-Chervonenkis theory (VC) control of the number of support vectors and margin. Although SVR is not as widespread as SVM, yet it has been used in multiple areas and a variety of researches, including but not limited to; control systems, bioinformatics, electric loads and consumption, customer demand, finance, tourism demand, air quality, prices in the market, and flood control [38].

The SVR model parameters considered in the MATLAB 2018 software are presented in Table 9.

The UCS results predicted by the SVR model are shown in Fig. 13 and compared with the actual mode. The comparison indicates that the SVR model has presented a good accuracy in the UCS prediction. The R<sup>2</sup> value of 0.9363 in Fig. 14, and the other statistical indices results in Table 10, show the good ability of the SVR model in the UCS prediction considering the database applied in this study.

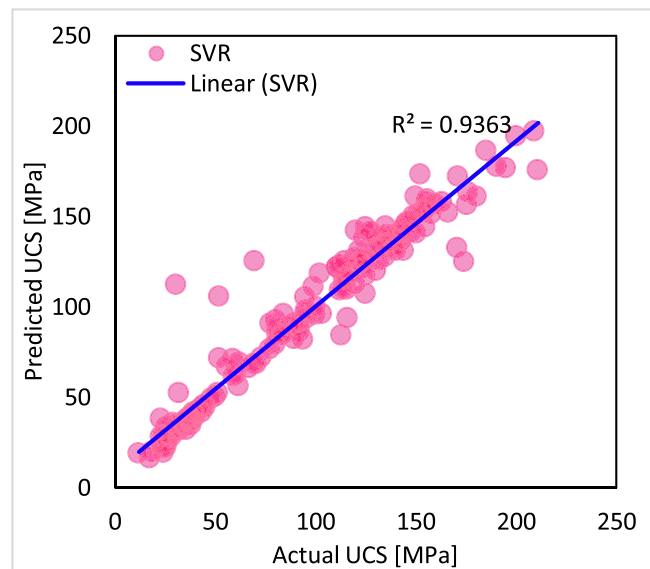
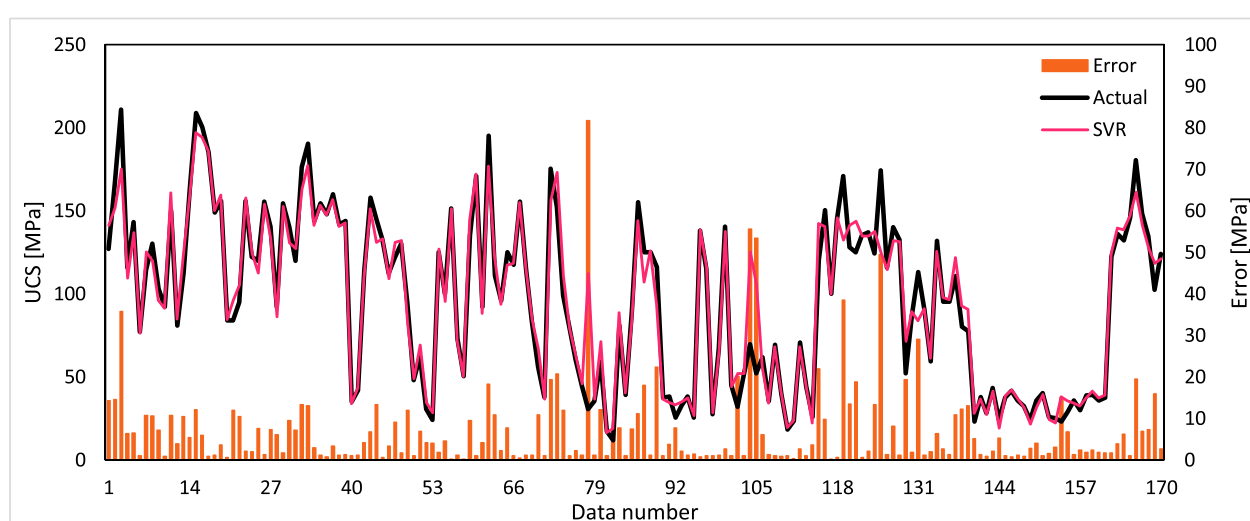
### DT

Decision Tree (DT) is one of the most practical and renowned

techniques for supervised learning. As it is already mentioned for the algorithms discussed above, DT has two types; DT Classifier and DT Regressor. While the working principles and features are pretty much similar in both of the classes. The algorithm works in a tree structure and breaks down the dataset into smaller subsets, then breaking down the subsets into smaller and smaller subsets until it reaches the final stage. The tree cannot be broken down any further. The tree has two main parts: first, decision nodes with at least two branches representing the values for the attribute tested, and second, leaf nodes represent the decision to the final numerical target (Fig. 15).

The DT model parameters considered in the MATLAB 2018 are described in Table 11.

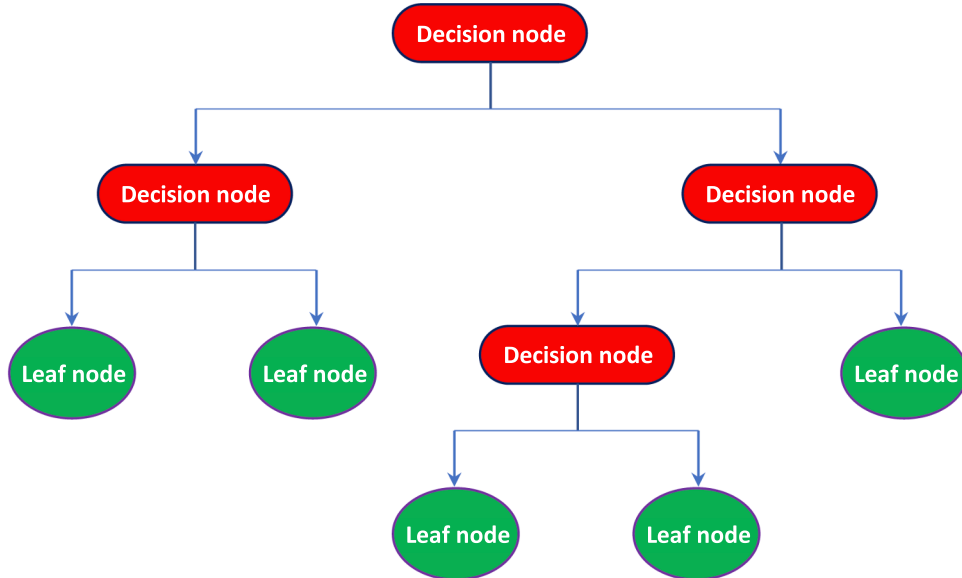
The UCS results predicted by the DT model are shown in Fig. 16 and compared with the measured UCS values. Looking at Fig. 16, the DT

**Fig. 14.** Prediction performance of SVR method on UCS prediction.**Fig. 13.** UCS prediction results of the SVR model.

**Table 10**

Evaluation criteria results of the SVR model.

R <sup>2</sup>	MAE	MSE	RMSE	RRMSE	MAPE [%]	MRE
0.9363	8.42E-02	1.204178113	1.097350497	0.008640555	0.066270032	0.0006627

**Fig. 15.** DT learning process.**Table 11**

Parameters of the DT model considered by MATLAB 2018 software.

Parameter	Value or type
Model type	'Fine Tree'
'PredictorSelection' — Algorithm used to select the best split predictor	'allsplits'
SplitCriterion — Split criterion	'mse'
'Prune' — Flag to estimate the optimal sequence of pruned subtrees	'on'
'MaxNumSplits' — Maximal number of decision splits	169
'MinLeafSize' — Minimum number of leaf node observations	1
'MinParentSize' — Minimum number of branch node observations	10

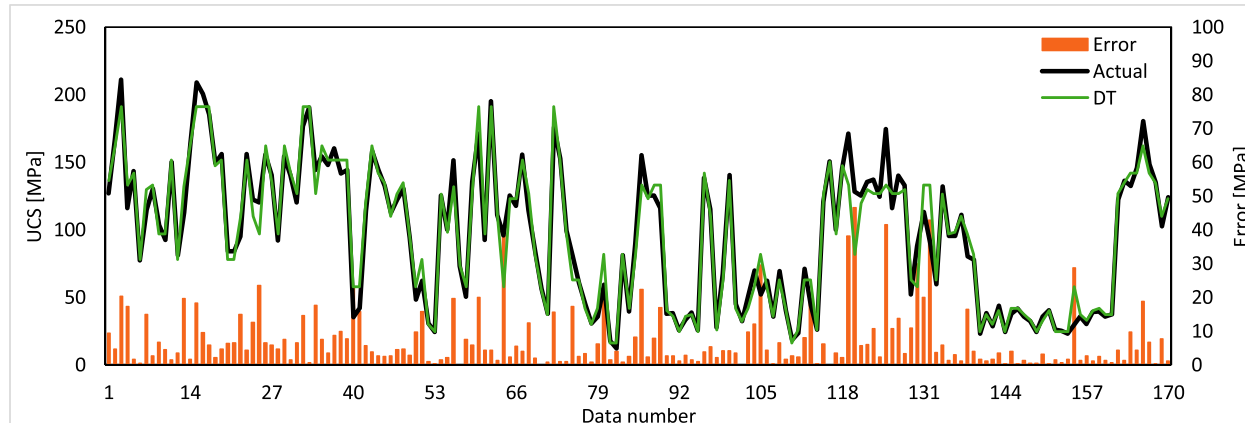
model results are in good agreement with the actual mode. This agreement is also seeable in the R<sup>2</sup> value in Fig. 17. Also, considering the database applied in this study, the other statistical indices results presented in Table 12 confirm the DT method's potential ability in the UCS

prediction.

### Results comparison

Looking at Fig. 18, according to the R<sup>2</sup> values, all the methods have provided significant accuracy. GPR has produced the best accuracy than the other models. In Fig. 19, the error values of the models are shown. According to Fig. 19, the dark blue color related to the GPR errors is less common than the other colors. All the other evaluation criteria in this study are presented in Table 13 for all the prediction models. According to these results, GPR has produced a perfect prediction accuracy. However, between the six model of LSTM, DNN, KNN, GPR, SVR and DT considered in this study for the UCS prediction, all the models can be suggested for UCS prediction of future researches. But, the GPR model results can be more acceptable and more calculable than the other models.

This study provides similar results compared to the other previous

**Fig. 16.** UCS prediction results of the DT model.

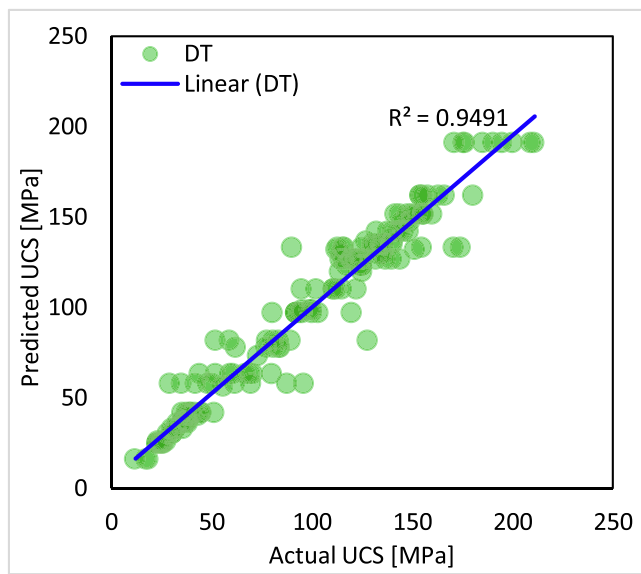


Fig. 17. Prediction performance of DT method on UCS prediction.

studies, in which the different parameters were considered to predict UCS using the different intelligent models. Most of the earlier research on the UCS prediction using the different artificial intelligent models is listed in Table 14 from 1999 to 2019. The UCS results predicted by the models considered in this study are also listed in Table 14. All the models' results are compared to each other through the  $R^2$  value. Table 14 shows that the more accurate prediction results are produced by the GPR model applied in this study. After the GPR model, artificial neural networks (ANN) and adaptive neuro-fuzzy inference system (ANFIS) models presented by Sarkar et al. [65], and Jahan Armaghani et al. [28], respectively, have produced more accurate results than the other models. However, it should be noted that in addition to the type of forecast model, the type of data, the number of data, and the type and number of the considered features affective on the UCS, also affect the results. Also, the number of data intended for training and testing is very important. In the previous studies, several data were used for training and the other number for testing. But, if the data sets train is replaced by the other data sets, the results can change and the accuracy can be significantly reduced. In this study, the 5-fold CV method has been used in which all the data sets will have the experience of training and testing. In this case, if a new data set is added to the previous data, still a good prediction accuracy can be expected.

To check the generalization capacity of the GPR model, we selected three constant values for three inputs of all, and we changed the other input from minimum to maximum based on the database used in this study. Then, as in Fig. 20, the correlation between the GPR model output (UCS) and each input parameter was obtained. As shown in Fig. 20, by increasing the three parameters,  $I_s(50)$ ,  $V_p$ , and SH, the UCS parameter also increases. But as parameter  $n$  increases, the UCS parameter decreases. Therefore, the behavior shown here by the proposed prediction model between output and inputs is consistent with the actual state. In this way, the generalization of the proposed prediction model can be proved.

## Discussion and Conclusions

UCS parameter has a great deal of importance within rock mechanics applications such as tunnel and dam design, rock blasting and drilling, mechanical rock excavation and slope stabilization. The method for measuring UCS on a core sample has been standardized by both the American Society for Testing and Materials (ASTM) and the International Society for Rock Mechanics (ISRM). However, it is impossible to extract sufficient quantities of high-quality cores from weak, highly fractured, weathered and thinly bedded rocks. In addition, careful execution of this test is very difficult, time-consuming and expensive and involves destructive tests.

Due to these associated problems, and to save time and cost, the prediction of UCS using simpler indirect test methods as a function of rocks' physical and mineralogical properties through different statistical and multivariate techniques in practical perspective has been highlighted. However, it is approved that such correlations due to dependency and variation to rock types are not precise. Moreover, the identified drawbacks of statistical methods in the effectiveness of auxiliary factors, the uncertainty of experimental tests and inaccurate prediction in a wide expanded range of data should also be considered. According to characterized demerits, adopting other alternatives to overcome the associated problems in developing UCS predictive models is necessary. In such cases, artificial intelligence techniques have been approved as very beneficial tools to handle the uncertainties and insufficient data in modeling the material behavior from experimental data.

In recent years, a significant degree of success using soft computing and artificial intelligence-aided techniques than conventional statistical methods in producing more efficient UCS predictive models in rock engineering applications has been demonstrated.

In this article, six ML methods of LSTM, DNN, KNN, GPR, SVR, and DT were applied for prediction of UCS of different rock types by applying 170 data sets including four features of  $n$ , SH,  $V_p$ , and  $I_s(50)$ . For each of the ML methods, different model types were produced and finally, the best one was considered as the UCS prediction model. To

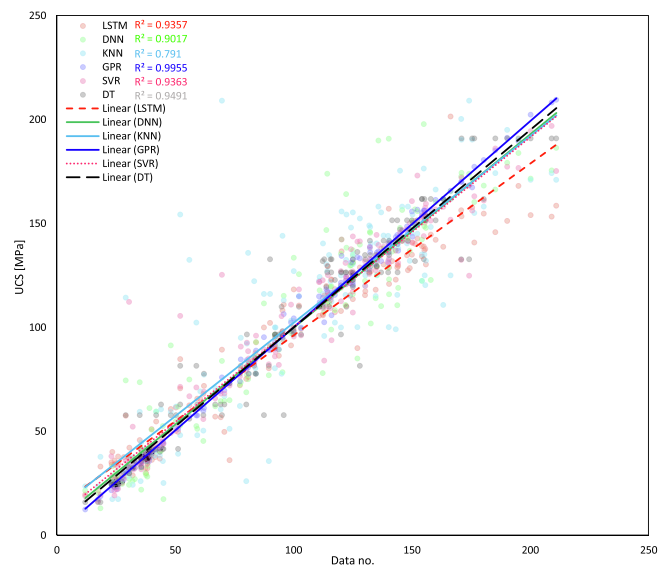
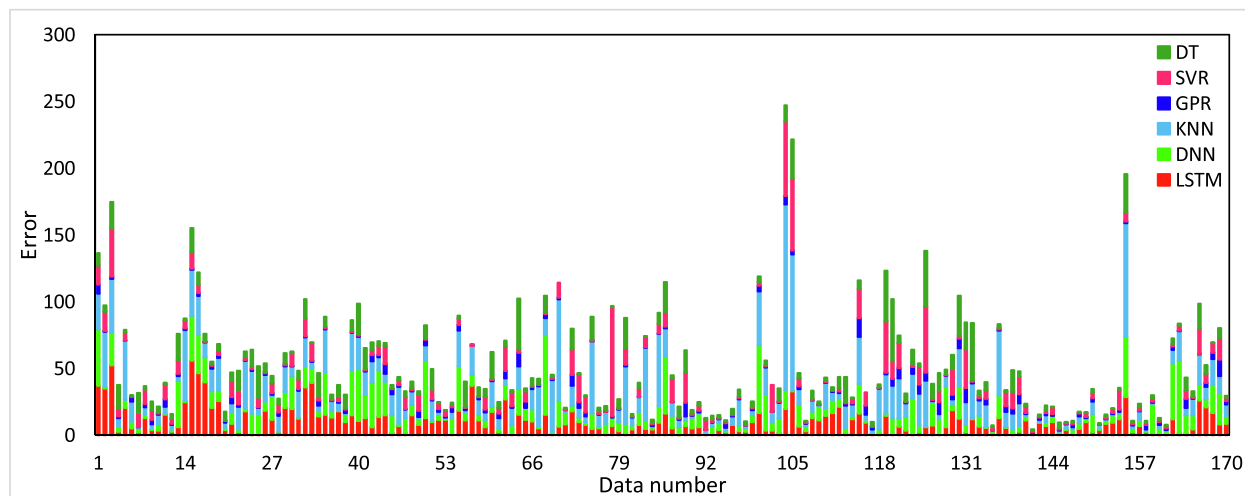


Fig. 18. Prediction performance of the intelligent methods on UCS prediction.

Table 12

Evaluation criteria results of the DT model.

$R^2$	MAE	MSE	RMSE	RRMSE	MAPE [%]	MRE
0.9491	5.44E-02	0.503853088	0.709826097	0.005589182	0.042867068	0.000428671



**Fig. 19.** A comparison between UCS prediction errors made by intelligent methods.

**Table 13**

A summary of the statistical evaluation criteria results made by the intelligent methods.

	LSTM	DNN	KNN	GPR	SVR	DT
R <sup>2</sup>	0.9357	0.9017	0.7910	0.9955	0.9363	0.9491
MAE	0.217647059	0.247058824	0.158294118	0.040011765	0.084162941	0.054441176
MSE	8.052941176	10.37647059	4.259694706	0.272160024	1.204178113	0.503853088
RMSE	2.837770459	3.221252953	2.063902785	0.521689585	1.097350497	0.709826097
RRMSE	0.022344649	0.025364196	0.016251203	0.004107792	0.008640555	0.005589182
MAPE	0.171375637	0.194534507	0.124641038	0.031505327	0.066270032	0.042867068
MRE	0.001713756	0.001945345	0.00124641	0.000315053	0.0006627	0.000428671

evaluate the performance ability of the ML models, the 5-fold CV method was used. The ML models' 5-fold CV results were compared to each other through different statistical evaluation criteria. The comparisons indicated the more ability of the GPR model than the other models with  $R^2$  of 0.9955 and RMSE of 0.52169. Also, a comparison was made between the ML models and the previous ML models done by the other researchers in UCS prediction from 1999 to 2019. Finally, it was concluded that the ML models applied in this study presented more accurate results than most of the previous works. Also, due to the employment the more data sets than the other researches and applying the K-fold CV method in the models, it was concluded that the results obtained by the ML models in this study are more acceptable and more reliable than the historical studies in the field.

In order to show how these models are used in practice, we assume that we want to determine the resistance status of the tunnel path rocks by calculating the UCS parameter before starting to build a tunnel. For this purpose, through coring, samples of tunnel path stones are obtained. As mentioned above, it is impossible to extract sufficient quantities of high-quality cores from weak, highly fractured, weathered and thinly bedded rocks. In this case, it won't be easy to prepare standard samples to calculate the UCS parameter in a laboratory method, affecting the laboratory results. Also, the number of samples may be huge and using the laboratory method to calculate UCS will lead to a significant increase in time and cost. The UCS parameter can be calculated using other easier parameters to achieve and require less time and cost to solve it. This study's four input parameters are  $Is(50)$ ,  $n$ ,  $V_p$  and  $SH$ .

To apply the GPR model in practice, first all parameters should be normalized in range [-1, 1] intervals before modeling to minimize input and output differences. Then, all model parameters must be considered in the MATLAB software. In this way, after running the model, the values of the UCS parameter can be predicted.

## Declaration of Competing Interest

The authors declare that they have no known competing financial interests or personal relationships that could have appeared to influence the work reported in this paper.

## References

- [1] Altindag R. Correlation between P-wave velocity and some mechanical properties for sedimentary rocks. *J. South Afr. Inst. Min. Metall.* 2012;112:229–37.
- [2] Abbaszadeh Shahri A, Larsson S, Johansson F. Updated relations for the uniaxial compressive strength of marlstones based on P-wave velocity and point load index test. *Innov. Infrastruct. Solut.* 2016;1:17. [https://doi.org/10.1007/s4106\\_016-0016-9](https://doi.org/10.1007/s4106_016-0016-9).
- [3] Asheghi R, Abbaszadeh Shahri A, Khorsand Zak M (2019) Prediction of Uniaxial Compressive Strength of Different Quarried Rocks Using Metaheuristic Algorithm. *Arab J Sci Eng* 2019;14:8645–59. <https://doi.org/10.1007/s13369-019-04046-8>.
- [4] Abdi Y, Garavand AT, Sahamieh RZ. Prediction of strength parameters of sedimentary rocks using artificial neural networks and regression analysis. *Arab J Geosci* 2018;11:587. <https://doi.org/10.1007/s12517-018-3929-0>.
- [5] Alvarez Grima M, Babuska R. Fuzzy model for the prediction of unconfined compressive strength of rock samples. *Int J Rock Mech. Min. Sci.* 1999;36:339–49.
- [6] Aydin A, Basu A. The Schmidt hammer in rock material characterization. *Eng. Geol.* 2005;81:1–14.
- [7] Ashtari M, Mousavi SM, Cheshomi A, Khamechiana M. Evaluation of the single compressive strength test in estimating uniaxial compressive and Brazilian tensile strengths and elastic modulus of marlstone. *Eng Geol* 2019;248:256–66. <https://doi.org/10.1016/j.jenggeo.2018.12.005>.
- [8] Baykasoglu A, Gullu H, Canakci H, Ozbakir L. Predicting of compressive and tensile strength of limestone via genetic programming. *Expert Syst Appl* 2008;35:111–23.
- [9] Beiki M, Majdi A, Givshad AD. Application of genetic programming to predict the uniaxial compressive strength and elastic modulus of carbonate rocks. *Int J Rock Mech Min Sci* 2013;63:159–69.
- [10] Barzegar R, Sattarpour M, Nikudel MR, Moghaddam AA. Comparative evaluation of artificial intelligence models for prediction of uniaxial compressive strength of travertine rocks, Case study: Azarshahr area, NW Iran. *Model. Earth Syst. Environ.* 2016;2:76. <https://doi.org/10.1007/s40808-016-0132-8>.
- [11] Çelik SB. Prediction of uniaxial compressive strength of carbonate rocks from nondestructive tests using multivariate regression and LS-SVM methods. *Arab J Geosci* 2019;12:193. <https://doi.org/10.1007/s12517-019-4307-2>.

**Table 14**

Comparison of the proposed models with other soft computing models reported in the literature.

**Table 14 (continued)**

References	Technic	Input	Output	Data set no.	R <sup>2</sup> for UCS
Mahdiabadi and Khanlari [54], Çelik [11], This study	RBF	Is <sub>(50)</sub> , RC, ρ, n, V <sub>p</sub> , WA	UCS	197	0.93
	GFFN	Is <sub>(50)</sub> , RC, ρ, n, V <sub>p</sub> , WA	UCS	197	0.95
	MLR	Is <sub>(50)</sub> , BPI, CPI	UCS, E	80	0.73
	MNLR	Is <sub>(50)</sub> , BPI, CPI	UCS, E	80	0.737
	ANN	Is <sub>(50)</sub> , BPI, CPI	UCS, E	80	0.782
	ANFIS	Is <sub>(50)</sub> , BPI, CPI	UCS, E	80	0.793
	MR	CSS, SH, V <sub>p</sub>	UCS	90	0.781
	LS-SVM	CSS, SH, V <sub>p</sub>	UCS	90	0.867
This study	LSTM	Is <sub>(50)</sub> , n, SH, V <sub>p</sub>	UCS	170	0.9357
	DNN	Is <sub>(50)</sub> , n, SH, V <sub>p</sub>	UCS	170	0.9017
	KNN	Is <sub>(50)</sub> , n, SH, V <sub>p</sub>	UCS	170	0.7910
	GPR	Is <sub>(50)</sub> , n, SH, V <sub>p</sub>	UCS	170	0.9955
	SVR	Is <sub>(50)</sub> , n, SH, V <sub>p</sub>	UCS	170	0.9363
	DT	Is <sub>(50)</sub> , n, SH, V <sub>p</sub>	UCS	170	0.9491

**Note:** ANN: Artificial neural network; ER: Equotip reading;  $\rho$ : Density; n: Porosity; GS: Grain size; RT: Rock type; FIS: fuzzy inference system; PC: Petrographic composition;  $V_p$ : P wave velocity; BPI: Block punch index;  $I_{S(50)}$ : Point load index; TS: Tensile strength; SH: Schmidt hammer; CI: Cone indenter hardness; GP: Genetic programming; WA: Water absorption; WC: Water content; PD: Packing density; C: concave-convex; Q: Quartz content; SD: Slake durability index; CC: Clay content; UW: Unit weight; NG: Neuro-genetic;  $R_n$ : Schmidt hammer rebound number; R: Lithology type; ANFIS: Adaptive neuro-fuzzy inference system; SVR: support vector regression; PDI: P-durability index; W: Weathering grade; BTS: Brazilian tensile strength test; PSO: Particle swarm optimization; ICA: Imperialist competitive algorithm; PR: Poisson's ratio; SVM: Support vector machine; SFL: Sugeno fuzzy logic; MLP: Multi-layer perceptron; MFL: Mamdani fuzzy logic; RF: Random Forest; MLR: Multiple linear regression; GFFN: Generalized feed-forward neural network; RC: Rock class; RBF: Radial basis function; MNLR: Multiple non-linear regression; CPI: Cylinder punch index; MR: Multivariate regression analyses; LS-SVM: least square support vector machines.

- [12] Canakci H, Baykasoglu A, Gullu H. Prediction of compressive and tensile strength of Gaziantep basalts via neural networks and gene expression programming. *Neural Comput Appl* 2009;18:1031–41.
  - [13] Cevik A, Sezer EA, Cabalar AF, Gokceoglu C. Modeling of the uniaxial compressive strength of some clay-bearing rocks using neural network. *Appl Soft Comput* 2011; 11:2587–94.
  - [14] Ceryan N. Application of support vector machines and relevance vector machines in predicting uniaxial compressive strength of volcanic rocks. *J Afr Earth Sci* 2014; 100:634–44.
  - [15] Dehghan S, Sattari GH, Chehreh Chelgani S, Aliabadi MA. Prediction of uniaxial compressive strength and modulus of elasticity for travertine samples using regression and artificial neural networks. *Min Sci Technol* 2010;20:41–6.
  - [16] Elmo D, Donati D, Stead D. Challenges in the characterisation of intact rock bridges in rock slopes. *Eng Geol* 2018;245(1):81–96. <https://doi.org/10.1016/j.enggeo.2018.06.014>.
  - [17] Ferentinou M, Fakir M. An ANN Approach for the Prediction of Uniaxial Compressive Strength, of Some Sedimentary and Igneous Rocks in Eastern KwaZulu-Natal. Symposium of the International Society for Rock Mechanics 2017; 191:1117–25. <https://doi.org/10.1016/j.proeng.2017.05.286>.
  - [18] Ghasemi E, Kalhor H, Bagherpour R, Yagiz S. Model tree approach for predicting uniaxial compressive strength and Young's modulus of carbonate rocks. *Bull Eng Geol Environ* 2016. <https://doi.org/10.1007/s10664-016-0931-1>

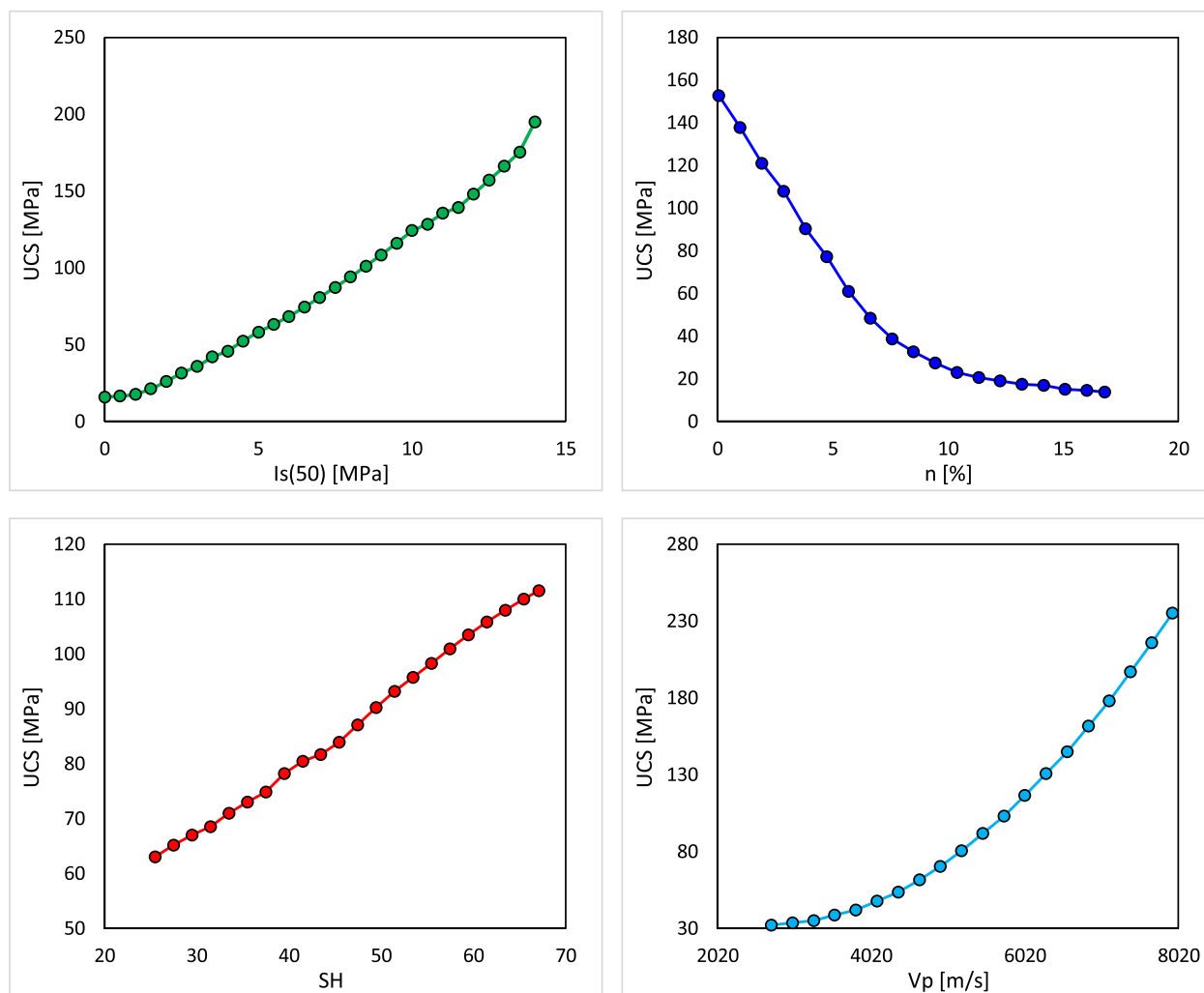


**Fig. 20.** Examining the generalization capacity of the GPR model.

- [19] Gokceoglu C, Zorlu K. A fuzzy model to predict the uniaxial compressive strength and the modulus of elasticity of a problematic rock. *Eng Appl Artif Intell* 2004;17: 61–72.
- [20] Gultekin NY, Gokceoglu C, Sezer EA. Prediction of uniaxial compressive strength of granitic rocks by various non-linear tools and comparison of their performances. *Int. J. Rock. Mech. Min. Sci.* 2013;62:113–22.
- [21] Gokceoglu C. A fuzzy triangular chart to predict the uniaxial compressive strength of Ankara agglomerates from their petro-graphic composition. *Eng Geol* 2002;66: 39–51.
- [22] Gokceoglu C, Sonmez H, Zorlu K. Estimating the uniaxial compressive strength of some clay-bearing rocks selected from Turkey by non-linear multivariable regression and rule-based fuzzy models. *Expert Syst* 2009;26:176–90.
- [23] Hu J, Wang J. Short-term wind speed prediction using empirical wavelet transform and Gaussian process regression. *Energy* 2015;93:1456–66.
- [24] Hosseini S, Al Khaled A (2014) A survey on the imperialist competitive algorithm metaheuristic: implementation in engineering domain and directions for future research. *Appl. Soft Comput. J.* 2014. <https://doi.org/10.1016/j.asoc.2014.08.024>.
- [25] Heidari M, Mohseni H, Jalali SH. Prediction of Uniaxial Compressive Strength of Some Sedimentary Rocks by Fuzzy and Regression Models. *Geotech Geol Eng* 2018; 36:401–12. <https://doi.org/10.1007/s10706-017-0334-5>.
- [26] Hochreiter S, Schmidhuber J. Long short-term memory. *Neural Comput* 1997;9(8): 1735–80.
- [27] Hannun AY, Rajpurkar P, Haghpanahi M, Tison GH, Bourn C, Turakhia MP, et al. Cardiologist-level arrhythmia detection and classification in ambulatory electrocardiograms using a deep neural network. *Nat Med* 2019;25(1):65.
- [28] Jahan Armaghani D, Tonnizam Mohamad E, Momeni E, Narayana-samy MS, Amin MFM. An adaptive neuro-fuzzy inference system for predicting unconfined compressive strength and Young's modulus: a study on Main Range granite. *Bull Eng Geol Environ* 2014;74:1301–19.
- [29] Jahan Armaghani D, Amin MFM, Yagiz S, Faradonbeh RS, Abdullah RA. Prediction of the uniaxial compressive strength of sandstone using various modeling techniques. *Int J Rock Mech Min Sci* 2016;85:174–86.
- [30] Jahan Armaghani D, Tonnizam Mohamad E, Momeni E, Monjezi M, Narayanasamy MS. Prediction of the strength and elasticity modulus of granite through an expert artificial neural network. *Arab J Geosci* 2016;9:48.
- [31] Kahraman S. Evaluation of simple methods for assessing the uniaxial compressive strength of rock. *Int. J. Rock Mech. Min. Sci.* 2001;38:981–94.
- [32] Kahraman S. The determination of uniaxial compressive strength from point load strength for pyroclastic rocks. *Eng. Geol.* 2014;170:33–42.
- [33] Kahraman S, Gunaydin O, Fener M. The effect of porosity on the relation between uniaxial compressive strength and point load index. *Int J. Rock Mech. Min. Sci.* 2005;42:584–9.
- [34] Kahraman S, Fener M, Gunaydin O. Estimating the uniaxial compressive strength of pyroclastic rocks from the slake durability index. *Bull Eng. Geol. Environ.* 2016. <https://doi.org/10.1007/s10064-016-0931-1>.
- [35] Karakus M, Tutmez B. Fuzzy and multiple regression modelling for evaluation of intact rock strength based on point load, Schmidt hammer and sonic velocity. *Rock Mech Rock Eng* 2006;39:45–57.
- [36] Kumar J, Goomer R, Singh AK. Long short term memory recurrent neural network (lstm-rnn) based workload forecasting model for cloud datacenters. *Procedia Comput Sci* 2018;125:676–82.
- [37] Lashkaripour GR. Predicting mechanical properties of mudrock from index parameters. *Bull. Eng. Geol. Environ.* 2002;61:73–7.
- [38] Lin KP, Pai PF, Lu YM, Chang PT. Revenue forecasting using a least-squares support vector regression model in a fuzzy environment. *Inf Sci* 2013;220:196–209.
- [39] Luo Y. Influence of water on mechanical behavior of surrounding rock in hard-rock tunnels: An experimental simulation. *Eng Geol* 2020;177:105816. <https://doi.org/10.1016/j.enggeo.2020.105816>.
- [40] Ling Y, Wang K, Wang X, et al. Prediction of engineering properties of fly ash-based geopolymer using artificial neural networks. *Neural Comput & Applic* 2019. <https://doi.org/10.1007/s00521-019-04662-3>.
- [41] Mahdiyar A, Armaghani DJ, Marto A, Nilashi M, Ismail S. Rock tensile strength prediction using empirical and soft computing approaches. *Bull Eng Geol Environ* 2019;78:4519–31. <https://doi.org/10.1007/s10064-018-1405-4>.

- [42] Meulenkamp F, Alvarez Grima M. Application of neural networks for the prediction of the unconfined compressive strength (UCS) from Equotip hardness. *Int J Rock Mech Min Sci* 1999;36:29–39.
- [43] Mishra DA, Srigyan M, Basu A, Rokade PJ. Soft computing methods for estimating the uniaxial compressive strength of intact rock from index tests. *Int. J. Rock Mech. Min. Sci.* 2015;80:418–24.
- [44] Monjezi M, Amini Khoshalan H, Razifard M. A neuro-genetic network for predicting uniaxial compressive strength of rocks. *Geotech Geol Eng* 2012;30: 1053–62.
- [45] Mishra D, Basu A. Estimation of uniaxial compressive strength of rock materials by index tests using regression analysis and fuzzy inference system. *Eng Geol* 2013; 160:54–68.
- [46] Majidi A, Rezaei M. Prediction of unconfined compressive strength of rock surrounding a roadway using artificial neural network. *Neural Comput & Appl* 2013;23:381–9.
- [47] Mahmoodzadeh A, Mohammadi M, Daraei A, Faraj RH, Mohammed Dler Omer RH, Sherwani AF. Decision-making in tunneling using artificial intelligence tools. *Tunn Undergr Space Technol* 2020;103:103514. <https://doi.org/10.1016/j.tust.2020.103514>.
- [48] Manouchehrian A, Sharifzadeh M, Hamidzadeh Moghadem R, Nouri T. Selection of regression models for predicting strength and deformability properties of rocks using GA. *Int J Min Sci Technol* 2013;23:495–501.
- [49] Mohamad ET, Zahed Armaghani D, Momeni E, Alavi Nezhad Khalil Abad SV. Prediction of the unconfined compressive strength of soft rocks: a PSO-based ANN approach. *Bull Eng Geol Environ* 2015;74:745–57.
- [50] Momeni E, Zahed Armaghani D, Hajihassani M, Amin MFM. Prediction of uniaxial compressive strength of rock samples using hybrid particle swarm optimization-based artificial neural networks. *Measurement* 2015;60:50–63.
- [51] Madhubabu N, Singh PK, Kainthola A, Mahanta B, Tripathy A, Singh TN. Prediction of compressive and elastic modulus of carbonate rocks. *Measurement* 2016;88: 202–13.
- [52] Mahmoodzadeh A, Mohammadi M, Daraei A, Farid Hama Ali H, Ismail Abdullah A, Kameran Al-Salihi N. Forecasting tunnel geology, construction time and costs using machine learning methods. *Neural Comput Appl* 2020. <https://doi.org/10.1007/s00521-020-05006-2>.
- [53] Matin SS, Farahzadi L, Makaremi S, Chelgani S Chehreh, Satari Gh. Variable selection and prediction of uniaxial compressive strength and modulus of elasticity by Random Forest. *Appl Soft Comput* 2018;70:980–7. <https://doi.org/10.1016/j.asoc.2017.06.030>.
- [54] Mahdiabadi N, Khanlari G. Prediction of Uniaxial Compressive Strength and Modulus of Elasticity in Calcarenous Mudstones Using Neural Networks, Fuzzy Systems, and Regression Analysis. *Periodica Polytechnica Civil Engineering* 2019; 63:104–14. <https://doi.org/10.3311/PPci.13035>.
- [55] Mahmoodzadeh A, Mohammadi M, Daraei A, Farid Hama Ali H, Kameran Al-Salihi N, Omer Mohammed Dler, et al. Forecasting maximum surface settlement caused by urban tunneling. *Autom Constr* 2020;120:103375. <https://doi.org/10.1016/j.autcon.2020.103375>.
- [56] Mahmoodzadeh A, Mohammadi M, Daraei A, Rashid TA, Sherwani AFH, Faraj RH, et al. Updating ground conditions and time-cost scatter-gram in tunnels during excavation. *Autom Constr* 2019;105:102822. <https://doi.org/10.1016/j.autcon.2019.04.017>.
- [57] Mahmoodzadeh A, Zare S. Probabilistic prediction of expected ground condition and construction time and costs in road tunnels. *J Rock Mech Geotech Eng* 2016;8: 734–45. <https://doi.org/10.1016/j.jrmge.2016.07.001>.
- [58] Nefeslioglu HA. Evaluation of geo-mechanical properties of very weak and weak rock materials by using non-destructive techniques: ultrasonic pulse velocity measurements and reflectance spectroscopy. *Eng. Geol.* 2013;160:8–20.
- [59] Palchik V. Influence of porosity and elastic modulus on uniaxial compressive strength in soft brittle porous sandstones. *Rock Mech. Rock Eng.* 1999;32:303–9.
- [60] Rezaei M, Majdi A, Monjezi M. An intelligent approach to predict unconfined compressive strength of rock surrounding access tunnels in longwall coal mining. *Neural Comput Appl* 2012;24(1):233–41.
- [61] Singh VK, Singh D, Singh TN. Prediction of strength properties of some schistose rocks from petrographic properties using artificial neural networks. *Int. J. Rock Mech. Min. Sci.* 2001;38:269–84.
- [62] Singh R, Umrao RK, Ahmad M, Ansari MK, Sharma LK, Singh TN. Prediction of geomechanical parameters using soft computing and multiple regression approach. *Measurement* 2017;99:108–19.
- [63] Singh R, Vishal V, Singh T, Ranjith PG. A comparative study of generalized regression neural network approach and adaptive neuro-fuzzy inference systems for prediction of unconfined compressive strength of rocks. *Neural Comput. Appl.* 2013;23:499–506. <https://doi.org/10.1007/s00522-012-0944-z>.
- [64] Sonmez H, Tuncay E, Gokceoglu C. Models to predict the uniaxial compressive strength and the modulus of elasticity for Ankara Agglomerate. *Int J Rock Mech Min Sci* 2004;41:717–29.
- [65] Sarkar K, Tiwary A, Singh TN. Estimation of strength parameters of rock using artificial neural networks. *Bull Eng Geol Environ* 2010;69:599–606.
- [66] Seifert C, Aamir A, Balagopalan A, Jain D, Sharma A, Grottel S, et al. Visualizations of deep neural networks in computer vision: A survey. In: *Transparent Data Mining for Big and Small Data*. Cham: Springer; 2017. p. 123–44.
- [67] Song Y, Liang J, Lu J, Zhao X. An efficient instance selection algorithm for k nearest neighbor regression. *Neurocomputing* 2017;251:26–34.
- [68] Tan X, Zhengbo H, Li W, Zhou S, Li T. Micromechanical Numerical Modelling on Compressive Failure of Recycled Concrete using Discrete Element Method (DEM). *Materials* 13(19):4329. Doi: 10.3390/ma13194329.
- [69] Tugrul A, Zarif IH. Correlation of mineralogical and textural characteristics with engineering properties of selected granitic rocks from Turkey. *Eng. Geol.* 1999;51: 303–17.
- [70] Yilmaz I, Sendir H. Correlation of Schmidt hardness with unconfined compressive strength and Young's modulus in gypsum from Sivas (Turkey). *Eng. Geol.* 2002;66: 211–9.
- [71] Tsiambaos G, Sabatakakis N. Considerations on strength of intact sedimentary rocks. *Eng. Geol.* 2004;72:261–73.
- [72] Taghavifar H, Mardani A, Taghavifar L. A hybridized artificial neural network and imperialist competitive algorithm optimization approach for prediction of soil compaction in soil bin facility. *Measurement* 2013;46:2288–99.
- [73] Tiriyaki B. Predicting intact rock strength for mechanical excavation using multivariate statistics, artificial neural networks, and regression trees. *Eng Geol* 2008;99:51–60.
- [74] Tonizam Mohamad E, Zahed Armaghani D, Momeni E, Alavi Nezhad Khalil Abad SV. Prediction of the unconfined compressive strength of soft rocks: a PSO-based ANN approach. *Bull Eng Geol Environ* 2014. <https://doi.org/10.1007/s10064-014-0638-0>.
- [75] Torabi-Kaveh M, Naseri F, Sanei S, Sarshari B. Application of artificial neural networks and multivariate statistics to predict UCS and E using physical properties of Asmari limestones. *Arab J Geosci* 2015;8:2889–97.
- [76] Wu CM, Schulz E, Speekenbrink M, Nelson JD, Meder B. Generalization guides human exploration in vast decision spaces. *Nat Hum Behav* 2018;2(12):915–24.
- [77] Williams, C. K., & Rasmussen, C. E. (2006). Gaussian processes for machine learning (Vol. 2, No. 3, p. 4). Cambridge, MA: MIT press.
- [78] Ying J, Han Z, Shen L, Li W. Influence of Parent Concrete Properties on Compressive Strength and Chloride Diffusion Coefficient of Concrete with Strengthened Recycled Aggregates. *Materials* 2020;13(20):4631. <https://doi.org/10.3390/ma13204631>.
- [79] Yu Y, Li W, Li J, Nguyen TN. A novel optimised self-learning method for compressive strength prediction of high performance concrete. *Constr Build Mater* 2018;184:229–47. <https://doi.org/10.1016/j.conbuildmat.2018.06.219>.
- [80] Yasar E, Erdogan Y. Correlating sound velocity with the density, compressive strength and Young's modulus of carbonate rocks. *Int. J. Rock Mech. Min. Sci.* 2004;41:871–5.
- [81] Yagiz S. Predicting uniaxial compressive strength, modulus of elasticity and index properties of rocks using Schmidt hammer. *Bull. Eng. Geol. Environ.* 2009;68: 55–63.
- [82] Yagiz S. Correlation between slake durability and rock properties for some carbonate rocks. *Bull. Eng. Geol. Environ.* 2011;70:377–83.
- [83] Yilmaz I, Yuksek AG. An example of artificial neural network (ANN) application for indirect estimation of rock parameters. *Rock Mech Rock Eng* 2008;41:781–95.
- [84] Yilmaz I, Yuksek G. Prediction of the strength and elastic modulus of gypsum using multiple regression, ANN, and ANFIS models. *Int J Rock Mech Min Sci* 2009;46: 803–10.
- [85] Yagiz S, Sezer EA, Gokceoglu C. Artificial neural networks and non-linear regression techniques to assess the influence of slake durability cycles on the prediction of uniaxial compressive strength and modulus of elasticity for carbonate rocks. *Int J Numer Anal Methods Geomech* 2012;36:1636–50.
- [86] Yesiloglu-Gultekin N, Sezer EA, Gokceoglu C, Bayhan H. An application of adaptive neuro fuzzy inference system for estimating the uniaxial compressive strength of certain granitic rocks from their mineral contents. *Expert Syst Appl* 2013;40:921–8.
- [87] Zorlu K, Gokceoglu C, Ocakoglu F, Nefeslioglu HA, Acikalin S. Prediction of uniaxial compressive strength of sandstones using petrography-based models. *Eng. Geol.* 2008;96:141–58.
- [88] Moradian OZ, Behnia M. Predicting the Uniaxial Compressive Strength and Static Young's Modulus of Intact Sedimentary Rocks Using the Ultrasonic Test. *Int. J. Geomechanics* 2009;9(1). [https://doi.org/10.1061/\(ASCE\)1532-3641\(2009\)9:1\(14\)](https://doi.org/10.1061/(ASCE)1532-3641(2009)9:1(14)).